



Munich Institute for
Astro- and Particle Physics

DECIPHERING STRONG-INTERACTION PHENOMENOLOGY THROUGH
PRECISION HADRON-SPECTROSCOPY

7 - 31 October 2019



Amplitude analysis (AA) at CMD-3 detector

Evgeny Kozyrev (on behalf of the CMD-3 collaboration)

BINP, NSU

e.a.kozyrev@inp.nsk.su

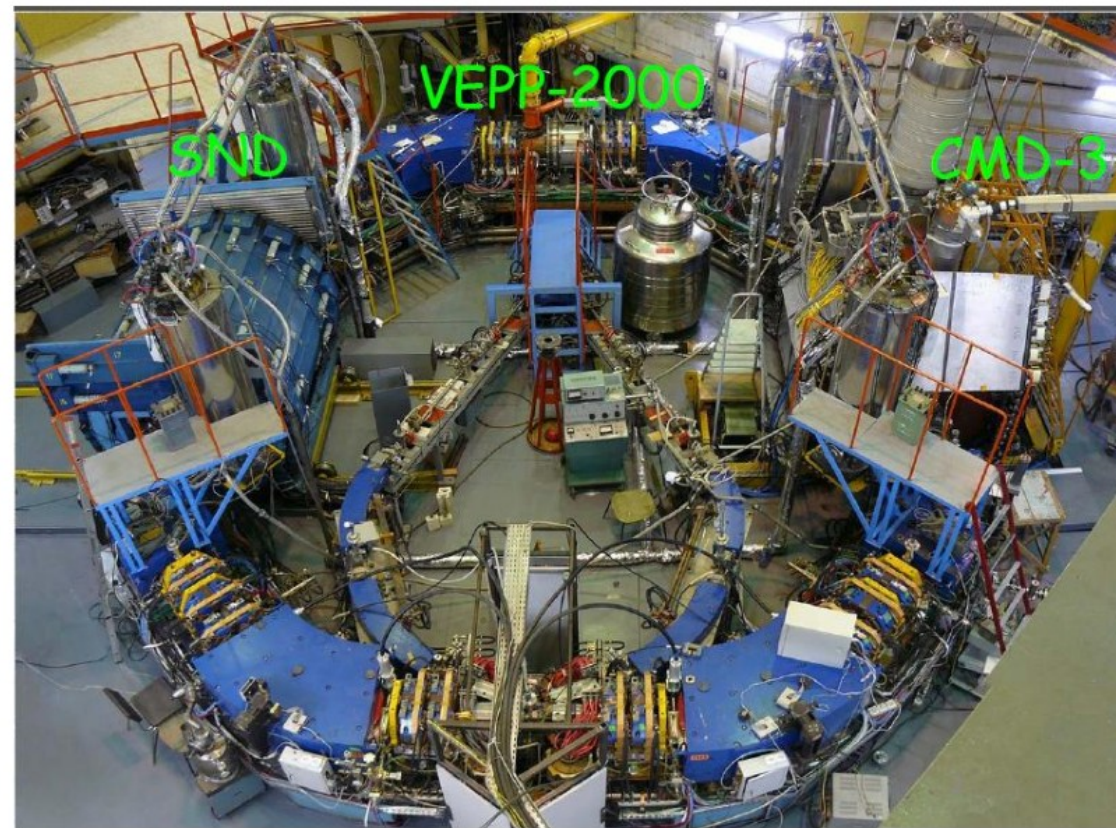
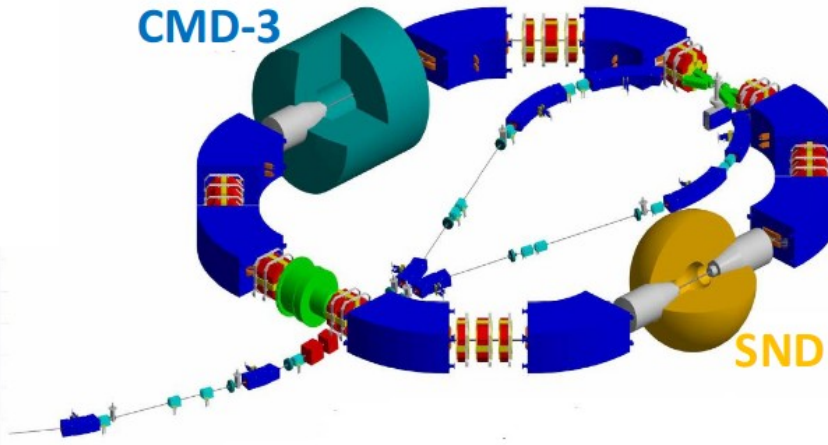
19.10.2019

Outline

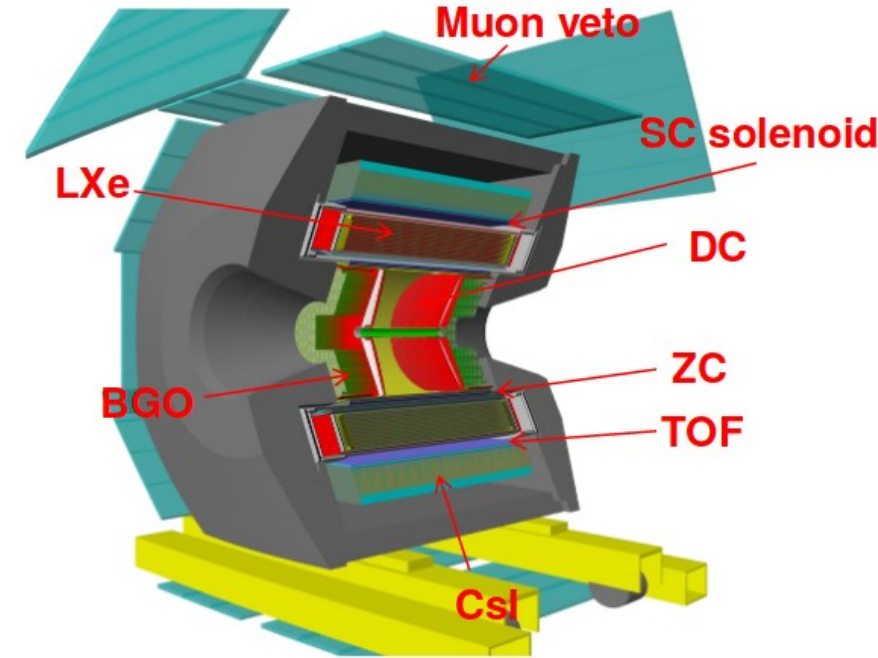
- recent results from the Cryogenic Magnetic Detector (CMD-3)
- $e^+e^- \rightarrow 4\pi$
- $e^+e^- \rightarrow K\bar{K}\pi\pi$

VEPP-2000

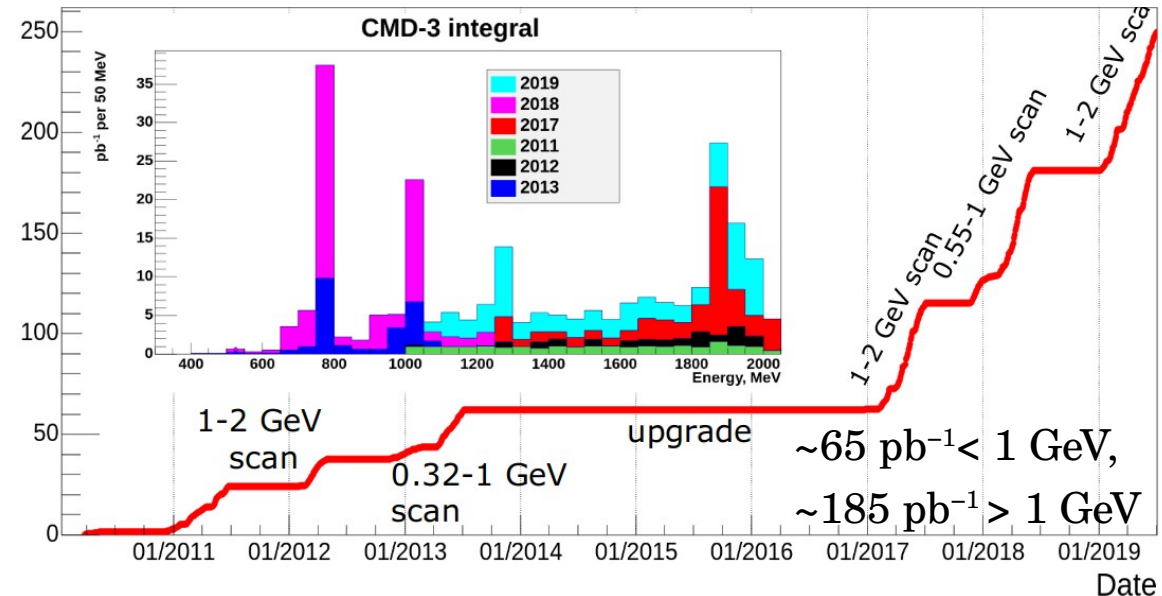
- VEPP-2000 (Novosibirsk, Russia) scans the \sqrt{s} in the range from 0.32 to 2.01 GeV
- Beam energy is monitored by the Compton backscattering laser light system with \sim 50 keV precision
- Uses “round beams” technique (focusing solenoids)
- Maximum luminosity achieved $4 \times 10^{31} \text{ cm}^{-2}\text{s}^{-1}$
- CMD-3 and SND detectors placed at two beam interaction points



CMD-3 detector & physics program



Collected 1/pb



- Precise measurement of $R = \sigma(e^+e^- \rightarrow \text{hadrons})/\sigma(e^+e^- \rightarrow \mu^+\mu^-)$ to achieve <1% systematic for major channels
- Study of the exclusive hadronic channels of e^+e^- annihilation, test of the isotopic relations
- Study of the “excited” vector mesons: ρ' , ρ'' , ω' , ϕ' ...
- Study of GE/GM for nucleons and behavior of hadronic cross sections near nucleon-antinucleon threshold
- CVC tests: comparison of isovector part of $\sigma(e^+e^- \rightarrow \text{hadrons})$ with τ -decays spectra
- Two-photon physics (e.g. η' production)

Exclusive channels of $e^+e^- \rightarrow hadrons$

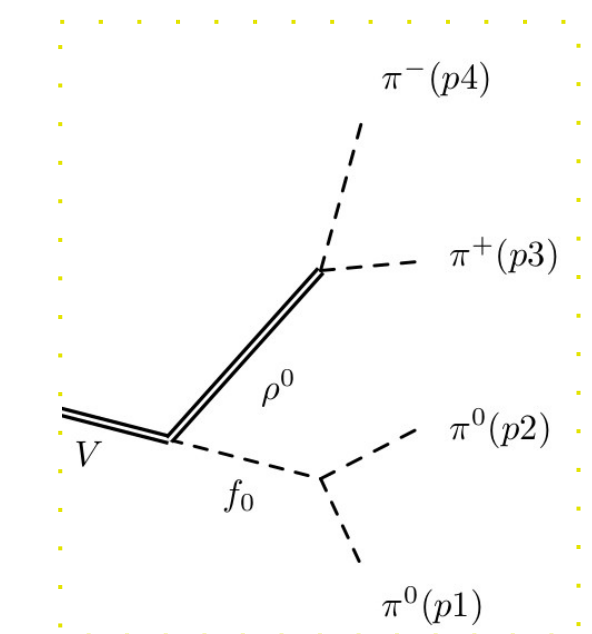
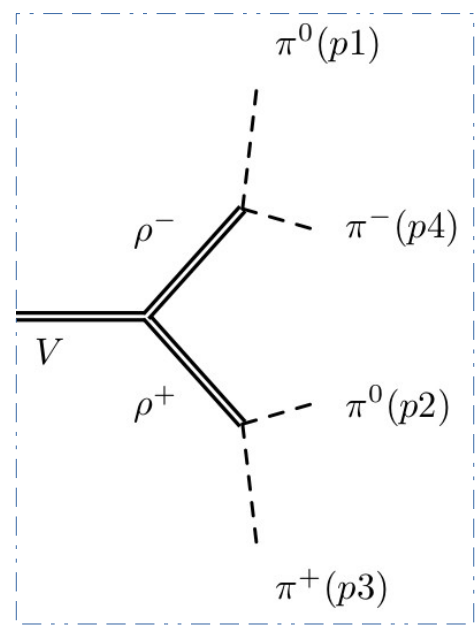
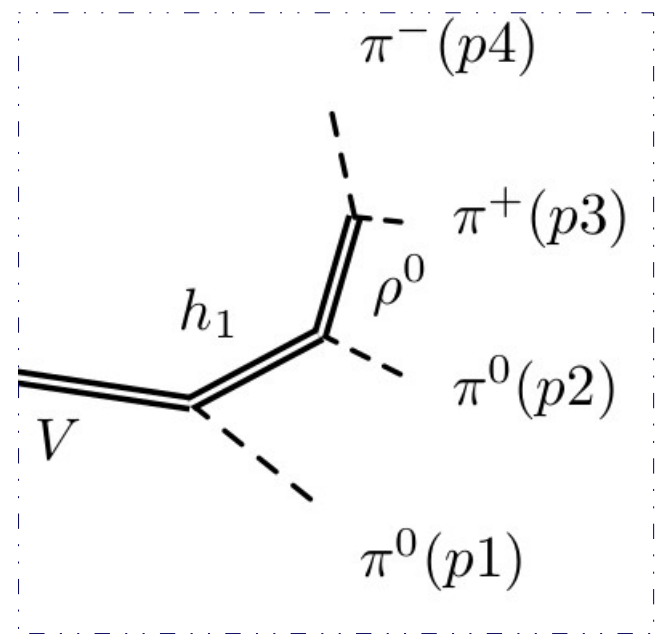
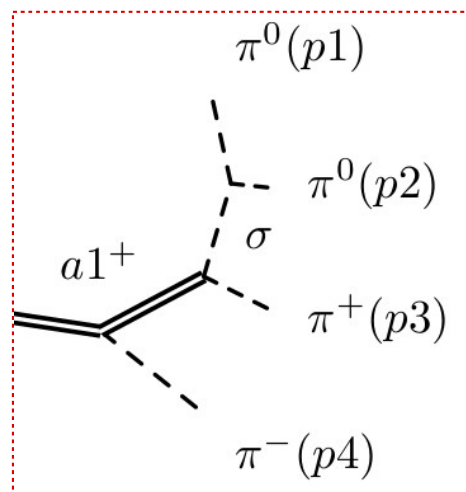
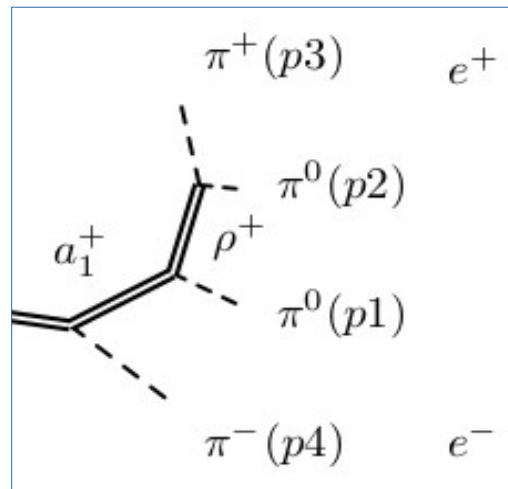
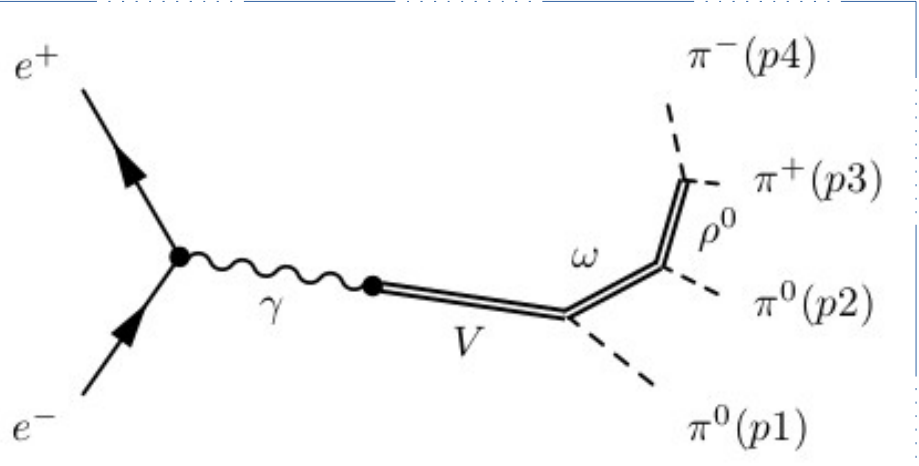
Event signature	Final state (published/submitted, in progress)					Published/submitted results:
2 charged	$\pi^+\pi^-$	K^+K^-	$KSKL$	pp	$\pi^+\pi^-\gamma$	$3\pi^+3\pi^-$: PLB 723 (2013) 82-89 η' : PLB 740 (2015) 273-277 $ppbar$: PLB 759 (2016) 634-640
2 charged + γ 's	$\pi^+\pi^-\pi^0$	$\pi^+\pi^-2\pi^0$	$\pi^+\pi^-3\pi^0$			$K^+K^-\pi^+\pi^-$: PLB 756 (2016) K^+K^- (at $\phi(1020)$): PLB 760 (2016) 314-319
4 charged	$2\pi^+2\pi^-$	$K^+K^-\pi^+\pi^-$	$KSK^\pm\pi^\mp$			$2\pi^+2\pi^-$ (near $\phi(1020)$): PLB 768 (2017) 345-350
4 charged + γ 's	$2\pi^+2\pi^-\pi^0$	$2\pi^+2\pi^-2\pi^0$				$\omega\eta$, $\eta\pi^+\pi^-\pi^0$: PLB 773 (2017) $KSKL$ (at $\phi(1020)$): PLB 779 (2018) 64-71
6 charged	$3\pi^+3\pi^-$	$KSKS\pi^+\pi^-$				$3\pi^+3\pi^-\pi^0$: PLB 792 (2019) $K^+K^-\eta$: PLB 798, (2019)134946
6 charged + γ 's	$3\pi^+3\pi^-\pi^0$					Observation of a fine structure
Fully neutral	$\pi^0\gamma$	$2\pi^0\gamma$	$3\pi^0\gamma$	$\eta\gamma$	$\pi^0\eta\gamma$...: PLB-D-19-00534R1
Other	nn	$\pi^0e^+e^-$	ηe^+e^-			

Outline for the next

- The study of $e^+e^- \rightarrow 4\pi$
- The study of $e^+e^- \rightarrow 2K2\pi$

Important remark

An amplitude analysis of reaction is interesting itself but also is required for the precise measurement of the cross section because of not 100% detector acceptance.



The amplitude analysis at CMD-2 (5.8 pb^{-1})

- The data in the $\text{ee} \rightarrow \pi^+\pi^-2\pi^0$ (22128 events) with $\sqrt{s} = [1.05\text{--}1.38] \text{ GeV}$ is used
- The dominance of the $\omega\pi$ and $a_1\pi$ is proved

Table 2

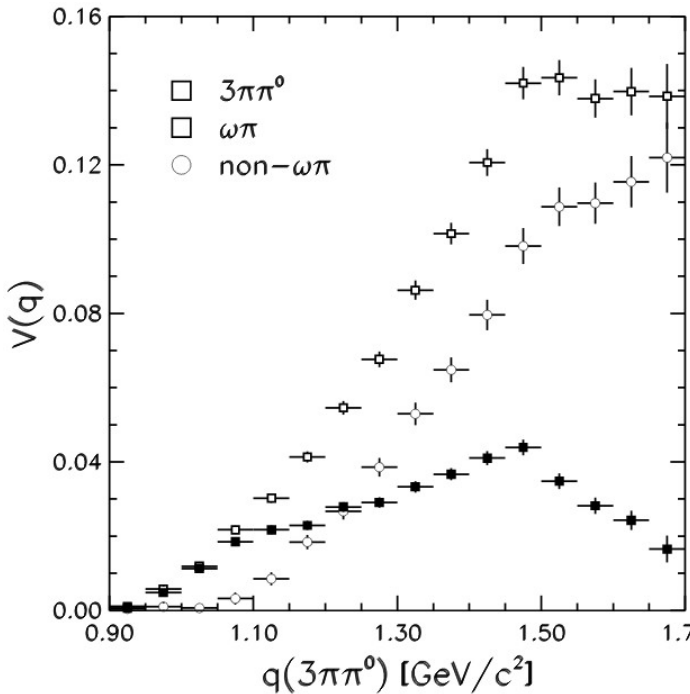
The results of a search for the admixture of other possible states

Model	L_{\min}	$r_X [\%]$	U.L. [%]
$\omega\pi^0 + a_1\pi$	1264	–	–
$\omega\pi^0 + a_1\pi + \rho\sigma$	1256	$2.1^{+1.2}_{-0.9}$	4.3
$\omega\pi^0 + a_1\pi + h_1\pi$	1263	$0.1^{+0.2}_{-0.1}$	0.4
$\omega\pi^0 + a_1\pi + a_2\pi$	1263	$0.2^{+0.4}_{-0.2}$	0.8
$\omega\pi^0 + a_1\pi + \pi'\pi$	1250	$9.5^{+3.2}_{-2.8}$	15.
$\omega\pi^0 + a_1\pi + \rho^+\rho^-$	1246	$4.7^{+2.0}_{-1.6}$	7.7

R.R. Akhmetshin et al., Physics Letters B **466** 1999 392–402

- The data in $\text{ee} \rightarrow \pi^+\pi^-2\pi^0$ and $\text{ee} \rightarrow 2\pi^+2\pi^-$ (28552) is used for the estimation: $B(a_1 \rightarrow \sigma\pi)/B(a_1 \rightarrow \rho\pi) \sim 0.3$

Amplitude analysis of $\tau \rightarrow 3\pi\pi^0\nu_\tau$ at CLEO (1999)



$$\frac{\Gamma(\tau^- \rightarrow \nu_\tau 2\pi^- \pi^+ \pi^0)}{\Gamma(\tau^- \rightarrow \nu_\tau e^- \bar{\nu}_e)} = \frac{3 \cos^2 \theta_c}{2\pi \alpha^2 m_\tau^8} \int_0^{m_\tau^2} dQ^2 Q^2 (m_\tau^2 - Q^2)^2 (m_\tau^2 + 2Q^2) \cdot \left[\frac{1}{2} \sigma_{e^+ e^- \rightarrow 2\pi^- 2\pi^+}(Q^2) + \sigma_{e^+ e^- \rightarrow \pi^+ \pi^- 2\pi^0}(Q^2) \right]$$

Model	Integrated amplitudes	Sum of amplitudes	Goodness-of-fit
Model 2	$R_{\omega\pi} = 0.38 \pm 0.02 \pm 0.02$ $R_{a_1\pi} = 0.43 \pm 0.02 \pm 0.02$	$0.81 \pm 0.03 \pm 0.03$	< 5%
Model 3	$R_{\omega\pi} = 0.38 \pm 0.02 \pm 0.01$ $R_{a_1\pi} = 0.49 \pm 0.02 \pm 0.02$ $R_{\sigma\rho} = 0.01 \pm 0.02 \pm 0.01$ $R_{f_0\rho} = 0.01 \pm 0.01 \pm 0.01$	$0.89 \pm 0.03 \pm 0.03$	20%

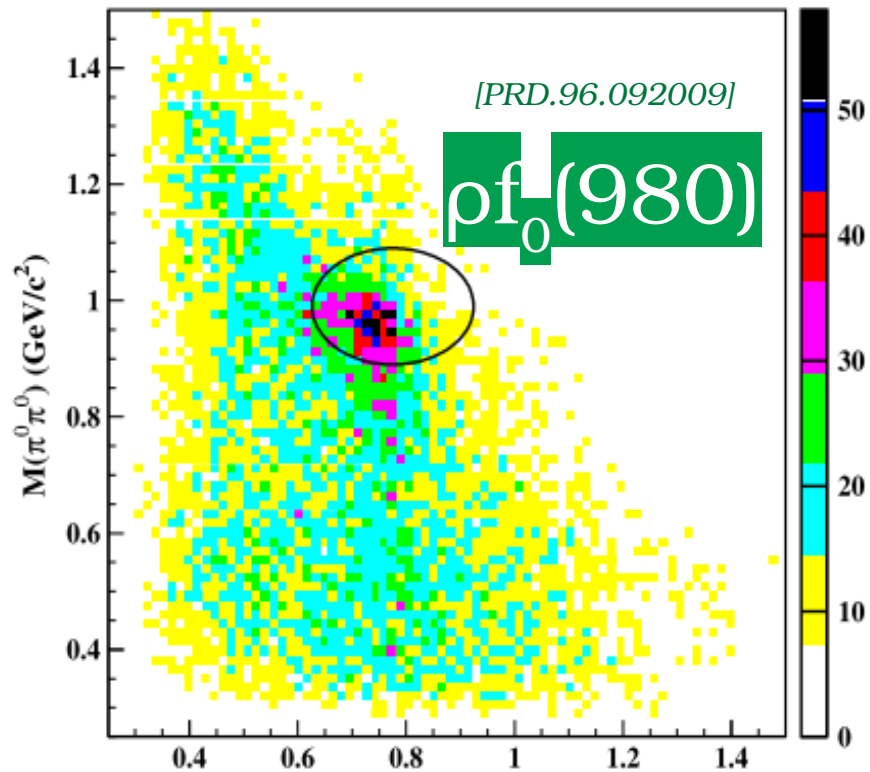
Spectral functions up to $m_{4\pi} < m_\tau$

Fit results for various models

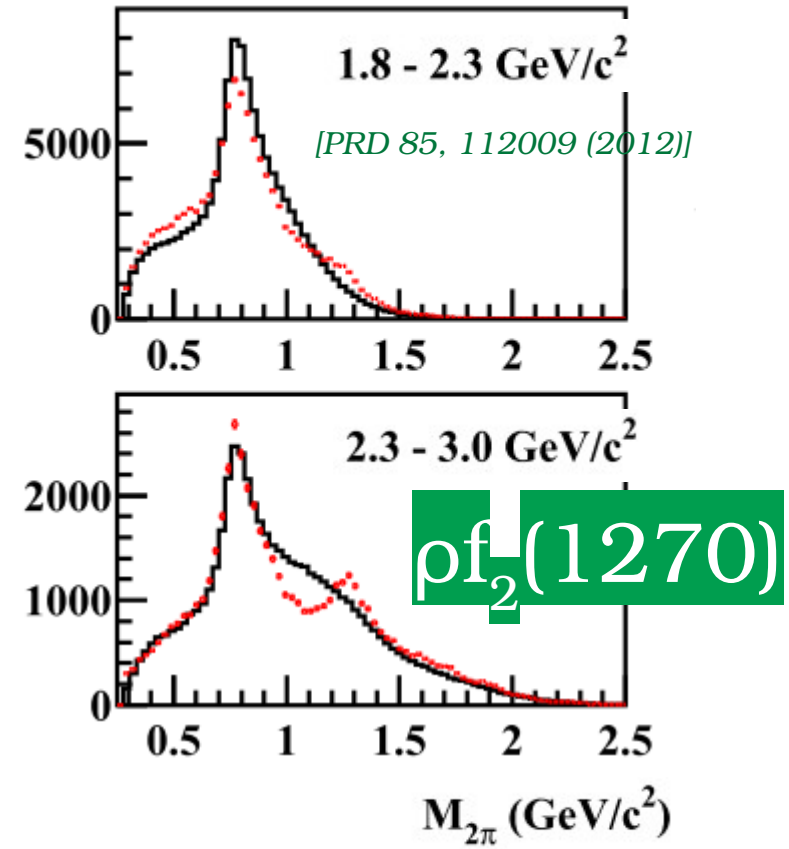
- Model with $\omega\pi$ and $a_1\pi$ and $\rho\sigma$, ρf_0 provides the best description of the data

Physical Review D - Particles, Fields, Gravitation and Cosmology, 61, 1-16 (2000).

The evidence of ρf_0 and ρf_2 with BaBar at $E_{\text{c.m.}} > 1.8 \text{ GeV}$



The evidence of $\rho f_0(980)$ in the process $e^+e^- \rightarrow 2\pi^0\pi^+\pi^-$ with BaBar



The evidence of $\rho f_2(1270)$ in the process $e^+e^- \rightarrow 2\pi^+\pi^-$ with BaBar ¹⁰

General strategy

Signal selection
 $(ee \rightarrow \pi^+\pi^- 2\pi^0)$

Signal selection
 $(ee \rightarrow 2\pi^+ 2\pi^-)$

amplitude construction by effective field theory

The minimization of likelihood function (L)

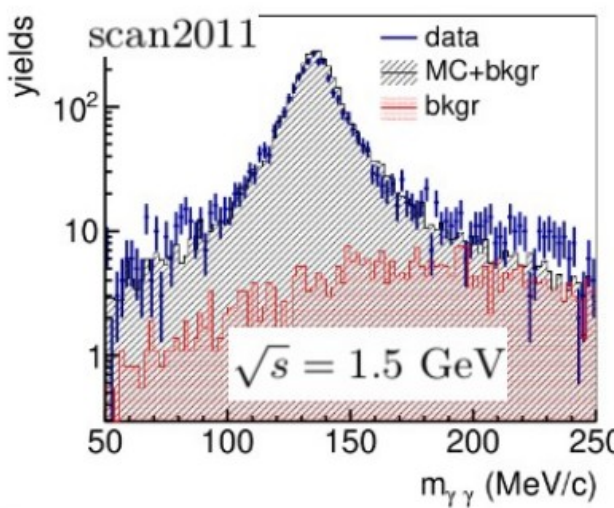
Model vs Experiment comparison

Systematic uncertainty

Event selection

(ee $\rightarrow \pi^+\pi^-2\pi^0$) 43 kevents

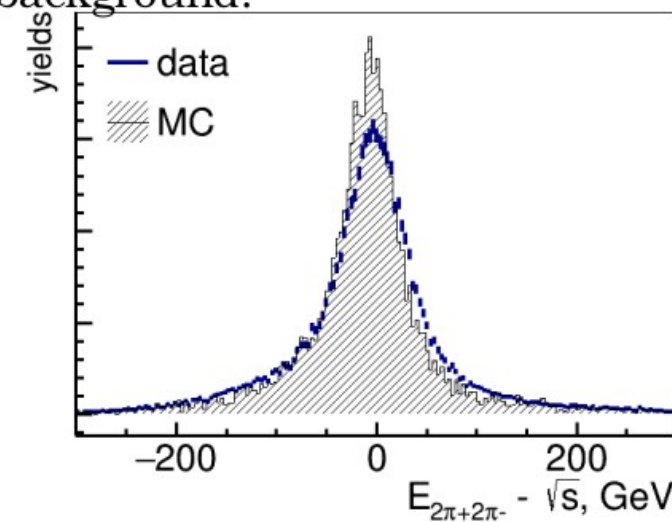
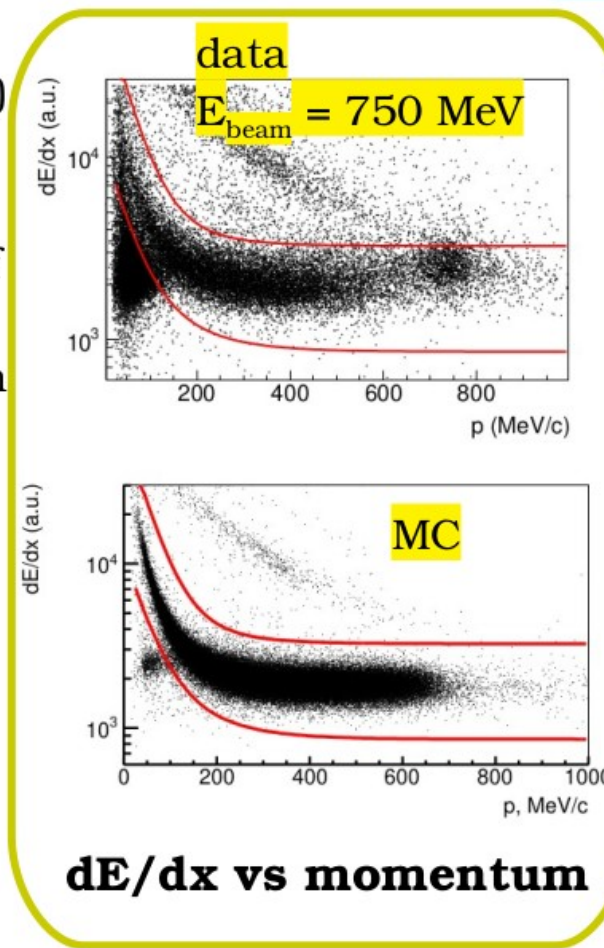
- $0.75 < \theta_{\pi,\gamma} < \pi - 0.75$ rad
- Total $E\sqrt{s}$ and $P < 150$ MeV/(c)
- Two candidates for π^0
- 6C kinematic fit
- The invariant mass spectrum of 3rd and 4th photons is used for the estimation of the contribution of background:



Event selection

(ee $\rightarrow 2\pi^+2\pi^-$) 83 kevents

- $0.75 < \theta_\pi < \pi - 0.75$ rad
- |Total $E| - \sqrt{s})$ and $P < 150$ MeV/(c)
- 4C kinematic fit
- The spectrum of total energy of four tracks ($E\sqrt{s}$) is used for the estimation of the contribution of background:



Amplitude analysis

The production of 4π system can proceed via a list of intermediate states:

- $\omega[1^{--}]\pi^0[0^{-+}]$ (only $2\pi^02\pi^\pm$)
- $a_1(1260)[1^+]\pi[0^-]$
- $\rho[1^{--}]f_0/\sigma[0^{++}]$
- $\rho f_2(1270)[2^{++}]$
- $\rho^+\rho^-$ (only $2\pi^02\pi^\pm$)
- $a_2(1320)[2^{++}]\pi$
- $h_1(1170)[1^{+-}]\pi^0$ (only $2\pi^02\pi^\pm$)
- $\pi'(1300)(0^{-+})\pi$

The relative number of events I at a particular point Ω in phase space can be represented as

$$I(\Omega) = |V_\alpha A_\alpha(\Omega)|^2$$

where the sum runs over all intermediate states, V_α - the complex production amplitude (the free parameter) and $A_\alpha(\Omega)$ - the amplitude at a particular point in phase space.

Amplitude analysis

The likelihood for model under test is

$$L = -\ln \prod_i \frac{|\sum_{\alpha} \mathbf{V}_{\alpha} A_{\alpha}^0(\Omega_i)|^2}{\frac{1}{N_{MC}^{gen}} \sum_k |\sum_{\alpha} \mathbf{V}_{\alpha} A_{\alpha}^0(\Omega_k)|^2} - \ln \prod_j \frac{|\sum_{\alpha} \mathbf{V}_{\alpha} A_{\alpha}^{\pm}(\Omega_j)|^2}{\frac{1}{N_{MC}^{gen}} \sum_k |\sum_{\alpha} \mathbf{V}_{\alpha} A_{\alpha}^{\pm}(\Omega_k)|^2},$$

The limited acceptance and efficiency of the detector is taken into account by summing only over simulated events that pass the reconstruction and analysis cuts.

- An amplitude is normalized to 1: $\int |A_{\alpha}(\Omega)|^2 d\Omega = 1$;
- The $\omega\pi^0$ amplitude is clearly seen at all energies, so $A_{\omega\pi^0}$ fixes at 1;
- C invariance: $A_{\alpha}^0(p_1, p_2, p_3, p_4) = -A_{\alpha}^0(p_1, p_2, p_4, p_3)$,
- Bose symmetry: $A_{\alpha}^0(p_1, p_2, p_3, p_4) = A_{\alpha}^0(p_2, p_1, p_3, p_4)$
- Gauge invariance: $q^{\mu} A_{\mu}(p_1, p_2, p_3, p_4) = 0$, where $q = p_{e^-} + p_{e^+}$.
- In the isospin limit: $A_{\alpha}^{\pm}(p_1(\pi^+), p_2(\pi^-), p_3(\pi^+), p_4(\pi^-)) = A_{\alpha}^0(p_1, p_2, p_3, p_4) + A_{\alpha}^0(p_3, p_2, p_1, p_4) + A_{\alpha}^0(p_1, p_4, p_3, p_2) + A_{\alpha}^0(p_3, p_4, p_1, p_2)$.

- Masses and central values of widths of resonances are fixed according to PDG.

- $T(1 \rightarrow 2 + 3) = \epsilon^{abc} \phi_1^a \phi_2^b \phi_3^c$, Isotopic structure $T(1 \rightarrow 2 + 3) = \delta^{ab} \phi_1^a \phi_2^b$

- $T(\rho\pi\pi) = g \cdot (p_{1\mu} - p_{2\mu}) \cdot \zeta_\mu \cdot \pi_1^\star \cdot \pi_2^\star$ $T(\sigma\pi\pi) = g \cdot \phi_1 \cdot \pi_1^\star \cdot \pi_2^\star$.

$$T(f_2\pi\pi) = g \cdot \omega_{\alpha\beta} p_{1\alpha} p_{2\beta} \delta^{ab} \phi_{\pi 1}^{\star a} \phi_{\pi 2}^{\star b}.$$

$$T(\rho' \omega \pi) = g_{\rho' \omega \pi} \epsilon^{\mu\nu\rho\sigma} \rho'_\mu W_\nu \omega_\rho^\star k_\sigma \delta^{ab} \phi_\pi^{\star a} \phi_{\rho'}^b,$$

$$T(\rho' a_1 \pi) = g_{\rho' a_1 \pi} (P_\mu \rho'_\nu - P_\nu \rho'_\mu) W_\mu a_{1\nu}^\star \cdot \epsilon^{abc} \phi_{\rho'}^a \phi_{a_1}^{\star b} \phi_\pi^{\star c},$$

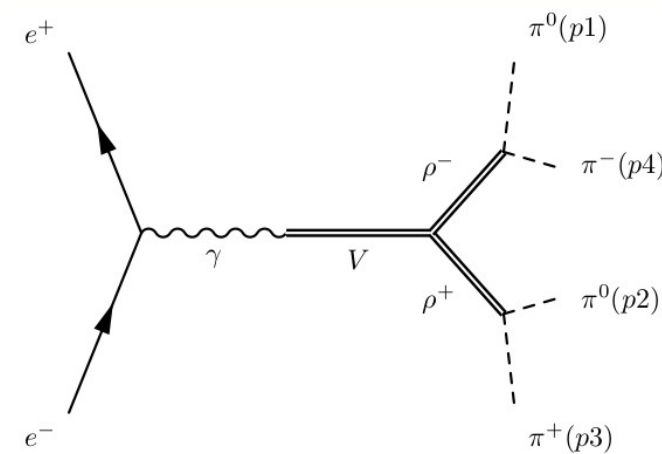
$$T(a_1 \sigma \pi) = g_{a_1 \sigma \pi} \cdot (W_\mu a_{1\nu} - W_\nu a_{1\mu}) k_\mu p_\nu \cdot \delta^{ab} \phi_{a_1}^a \phi_\pi^{\star b}.$$

$$T(\rho' \rho f_0) = g_{\rho' \rho f_0} \cdot (P_\mu \rho'_\nu - P_\nu \rho'_\mu) \cdot k_\mu \rho_\nu^\star \cdot \delta^{ab} \phi_{\rho'}^a \phi_\rho^{\star b}.$$

$$T(\rho' \rho f_2) = g_{\rho' \rho f_2} \cdot \rho'_\alpha \rho_\beta^\star \cdot \omega_{\alpha\beta}^\star \cdot \delta^{ab} \phi_{\rho'}^a \phi_\rho^{\star b}$$

$$T(\rho' h_1 \pi^0) = g_{\rho' h_1 \pi^0} \cdot (P_\mu \rho'_\nu - P_\nu \rho'_\mu) h_{1\mu}^\star W_\nu \cdot \delta^{ab} \phi_{\rho'}^a \phi_\pi^{\star b}$$

$$\begin{aligned} T(\rho' \rho^+ \rho^-) = & \left(g_{1\rho' \rho^+ \rho^-} \cdot \rho'_\mu Q_\mu \rho_\alpha^{+\star} \rho_\alpha^{-\star} + g_{2\rho' \rho^+ \rho^-} \cdot \rho'_\mu Q_\mu \rho_\alpha^{+\star} Q_\alpha \rho_\beta^{-\star} Q_\beta \right. \\ & \left. + g_{3\rho' \rho^+ \rho^-} \cdot (\rho'_\mu \rho_\mu^{+\star} Q_\alpha \rho_\alpha^{-\star} + \rho'_\mu \rho_\mu^{-\star} Q_\alpha \rho_\alpha^{+\star}) \right) \cdot \epsilon^{abc} \phi_{\rho'}^a \phi_{\rho^+}^{b\star} \phi_{\rho^-}^{c\star}, \end{aligned}$$

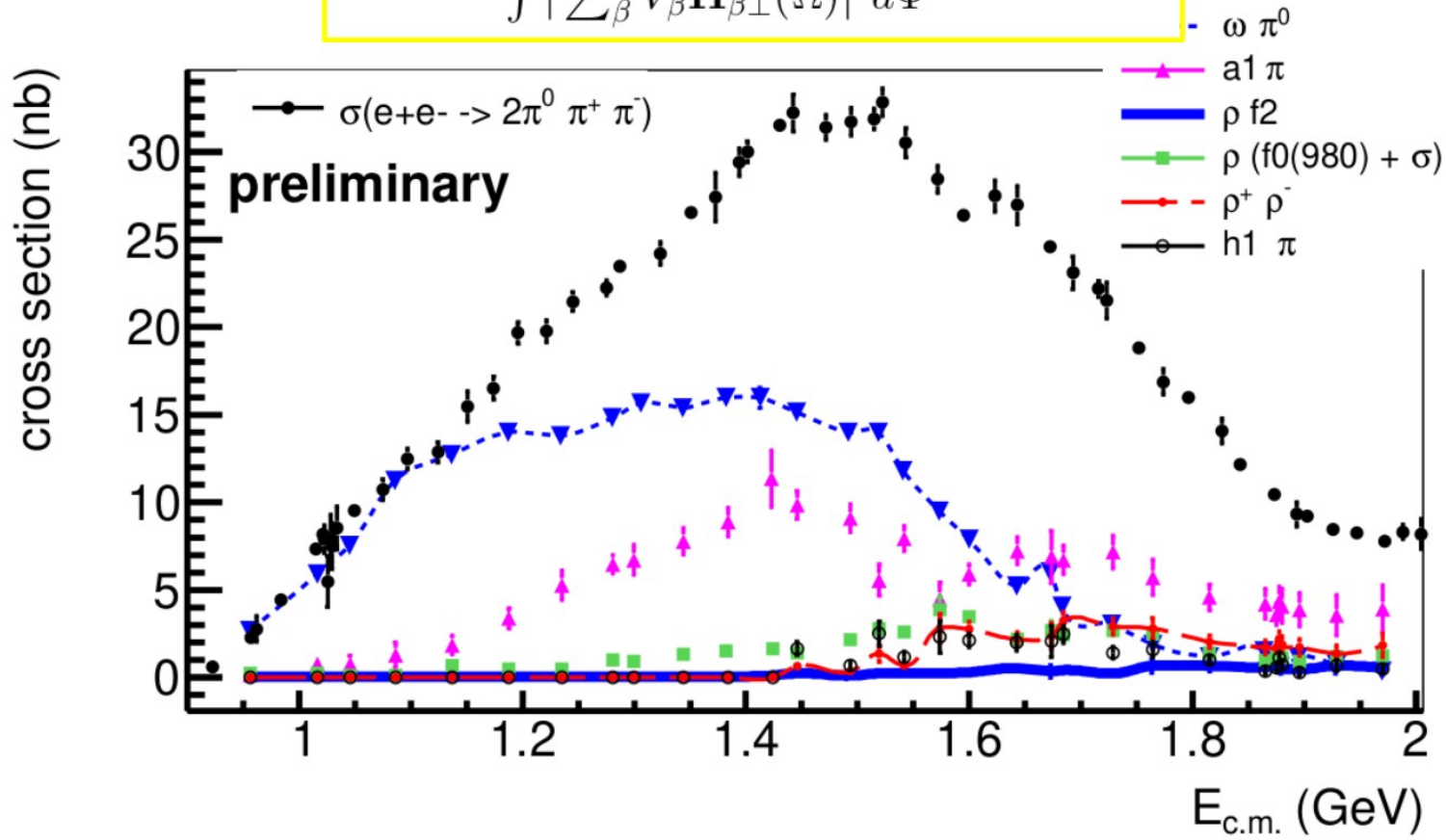


MIGRAD MINIMIZATION HAS CONVERGED.

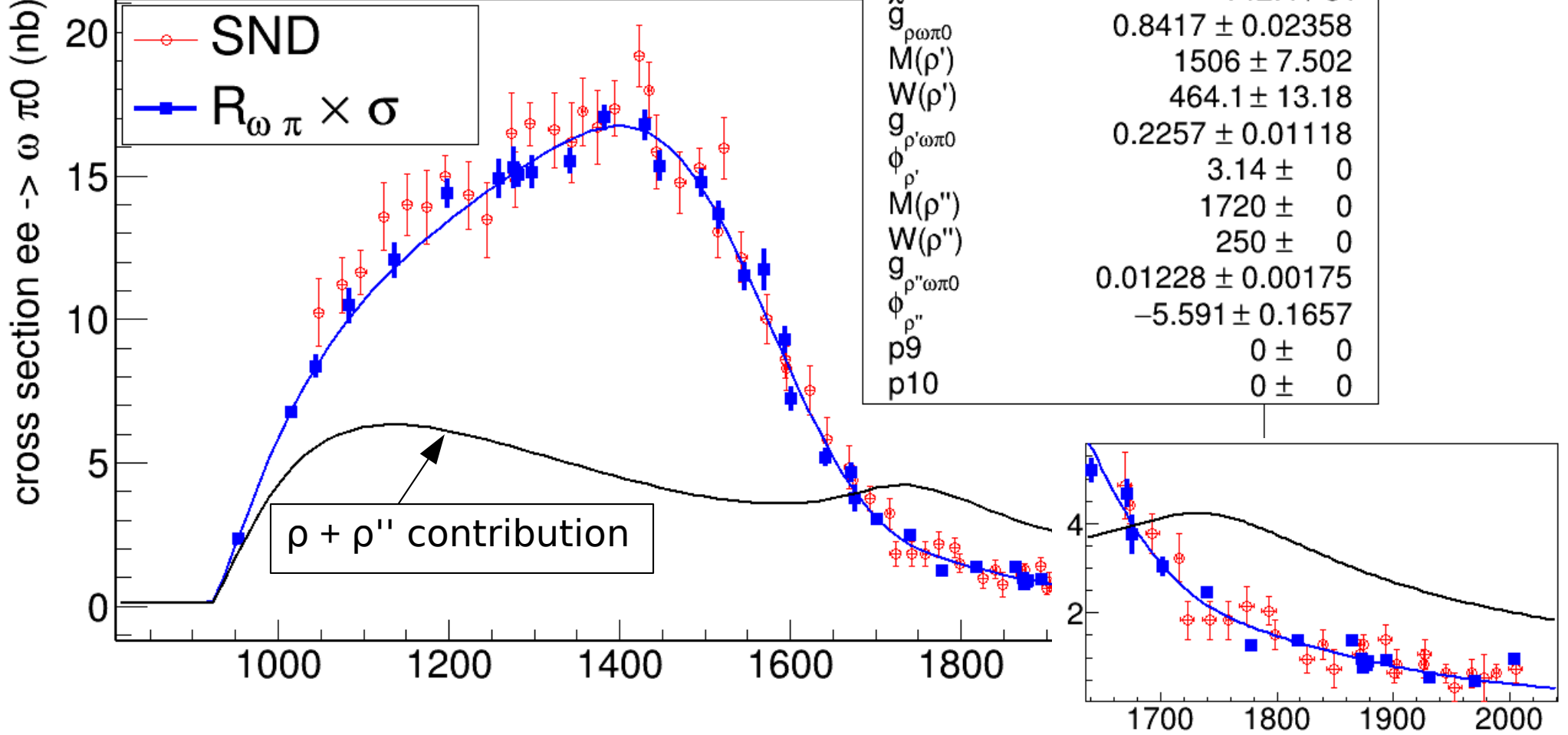
FCN=-3683.09 FROM MIGRAD STATUS=CONVERGED 1383 CALLS 2909 TOTAL
EDM=8.37303e-08 STRATEGY= 1 ERROR MATRIX UNCERTAINTY 2.6 per cent

EXT	PARAMETER	STEP	FIRST		
NO.	NAME	VALUE	ERROR	SIZE	DERIVATIVE
1	lambda	0.00000e+00	fixed		
2	ompi0	1.00000e+00	fixed		
3	a1 (rho pi)	3.71537e+00	1.13442e+00	-0.00000e+00	4.96594e-04
4	a1 (rho pi) phase	6.45875e+00	8.68014e-01	0.00000e+00	4.75273e-03
5	a1 (sigma pi)	1.90070e+00	4.18199e-01	0.00000e+00	-1.57770e-04
6	a1 (sigma pi) phase	7.04969e+00	2.45880e-01	0.00000e+00	-4.77347e-03
7	rho f0	1.07413e+00	3.80503e-01	-0.00000e+00	4.76961e-03
8	rho f0 phase	1.48534e+01	8.66400e-01	0.00000e+00	1.11573e-02
9	rhop rhom	0.00000e+00	fixed		
10	rhop rhom phase	5.10084e+00	fixed		
11	rho sigma	4.57957e+00	1.37645e+00	0.00000e+00	1.30840e-03
12	rho sigma phase	-1.16786e-01	8.98303e-01	0.00000e+00	-1.58780e-03
13	phase sp	0.00000e+00	fixed		
14	phase sp phase	0.00000e+00	fixed		
15	a2 pi	0.00000e+00	fixed		
16	a2 pi phase	0.00000e+00	fixed		
17	h1 pi	1.76724e+00	5.25981e-01	0.00000e+00	-1.64760e-04
18	h1 pi phase	2.16424e+01	8.35526e-01	0.00000e+00	-1.99606e-04
19	a1 (rho pi) pi_II	0.00000e+00	fixed		
20	a1 (rho pi) pi_II phase	0.00000e+00	fixed		
21	rho f0_inter	0.00000e+00	fixed		
22	rho f0_inter phase	0.00000e+00	fixed		
23	rho f2	1.72563e-01	5.34190e-02	-0.00000e+00	-3.33400e-02
24	rho f2 phase	-2.17129e+00	9.13877e-01	0.00000e+00	-6.29331e-03
25	rhop rhom II	1.34854e-01	5.09591e-02	-0.00000e+00	1.95684e-03
26	rhop rhom II phase	6.89196e-01	9.60407e-01	0.00000e+00	-8.70217e-03

$$R_i(s) = \frac{\int |V_i \cdot \mathbf{H}_{i\perp}(\Omega)|^2 d\Phi}{\int |\sum_{\beta} V_{\beta} \mathbf{H}_{\beta\perp}(\Omega)|^2 d\Phi} \cdot \sigma_{2\pi^0\pi^+\pi^-}(s)$$



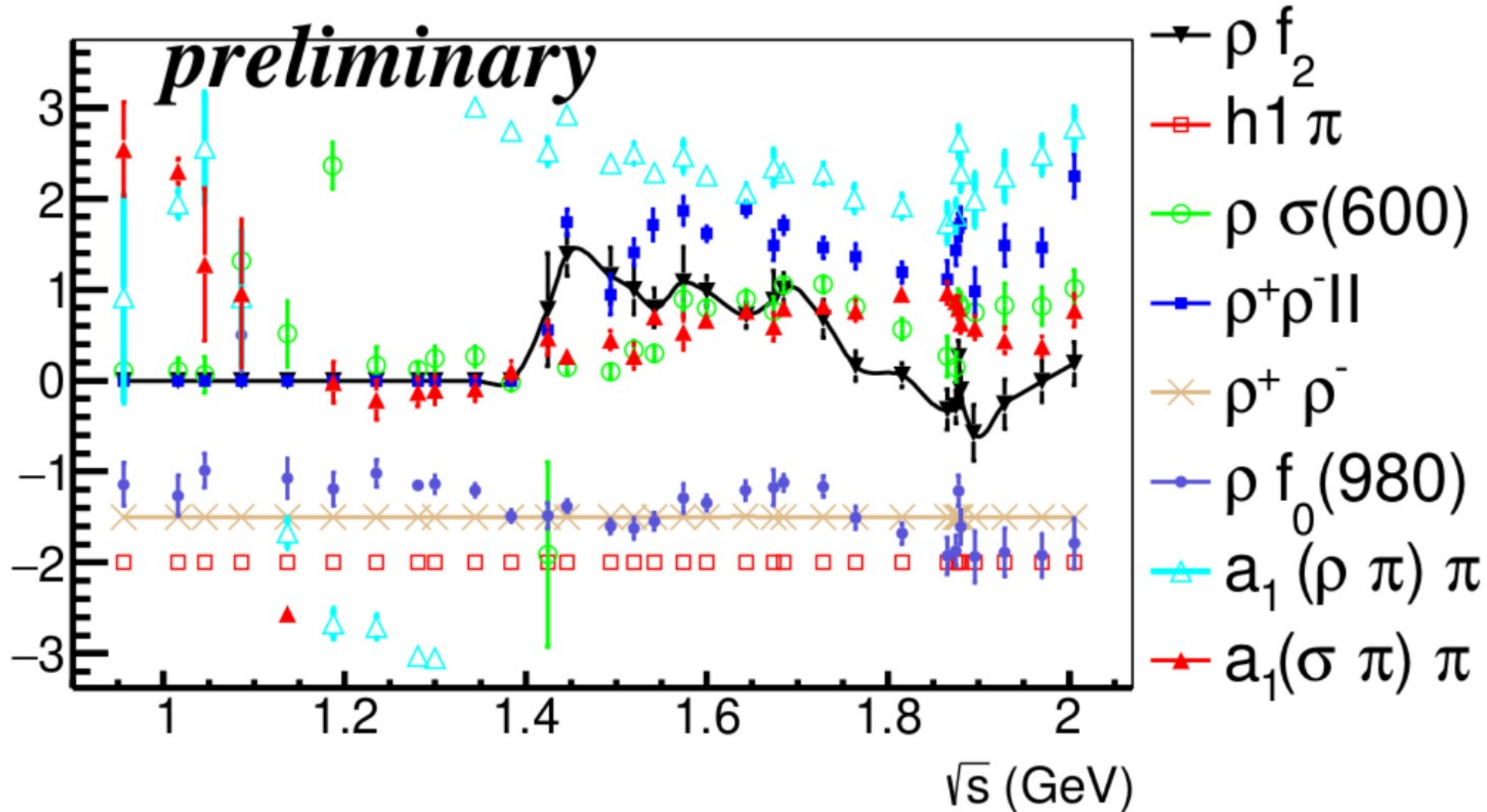
Obtained amplitudes can be used for the prediction of $W \rightarrow 4\pi$, ex., $\tau \rightarrow \omega\pi^-$, $\tau \rightarrow a_1(1260)\pi$, $\tau \rightarrow \rho^-[\sigma(500) + f_0(980)]$, $\tau \rightarrow \rho^- f_2(1270)$, $\tau \rightarrow \rho^- \rho^0$, $\tau \rightarrow h_1(1170)\pi^0$ ¹⁷



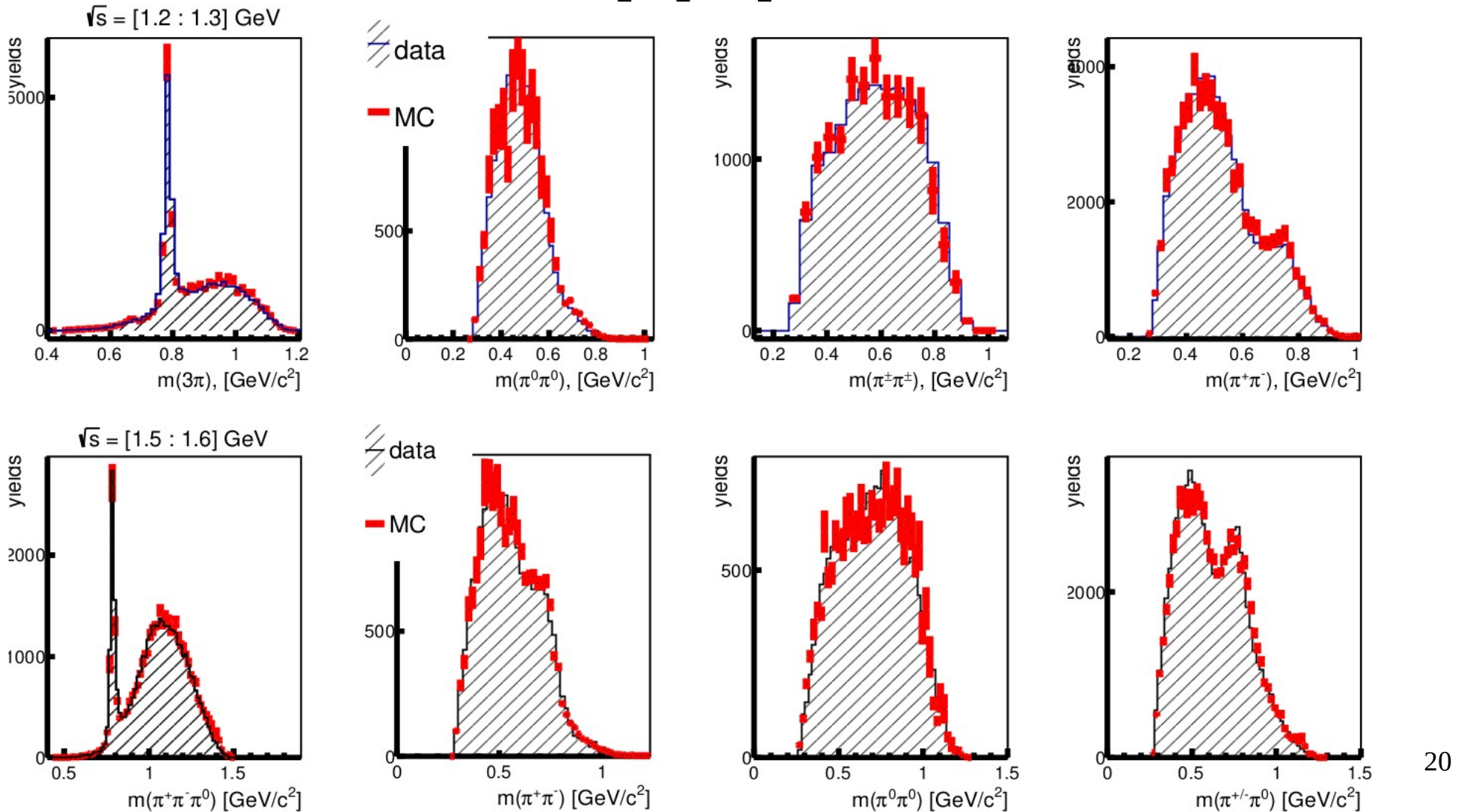
The cross-section of $e^+e^- \rightarrow \omega\pi^0$ vs $E_{\text{c.m.}}$

Phases of different amplitudes

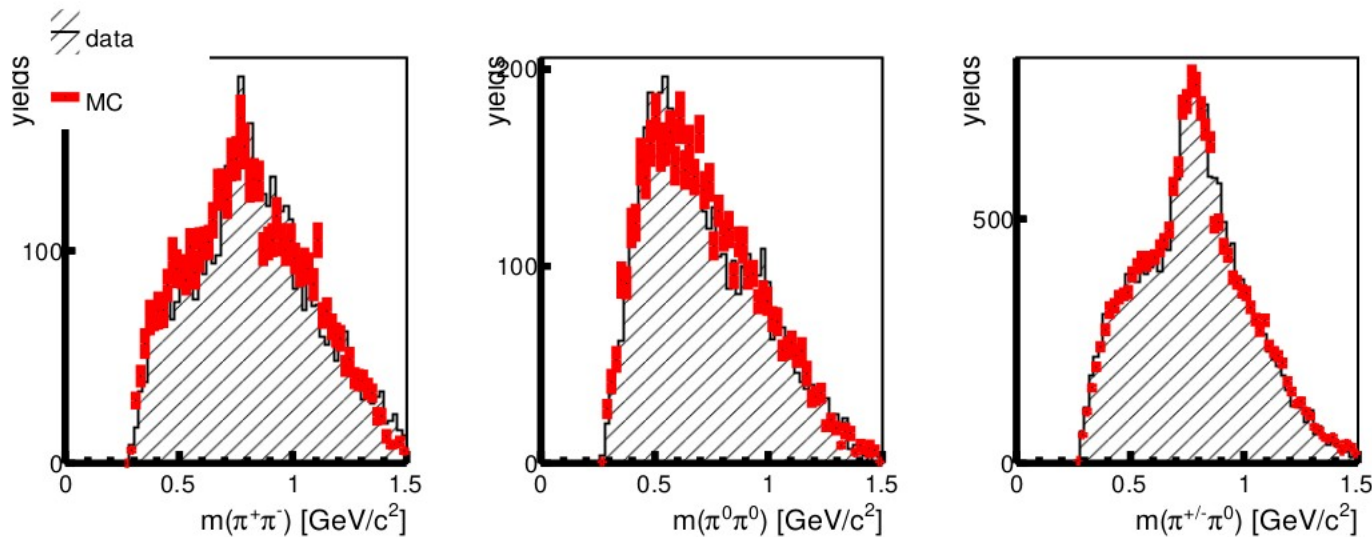
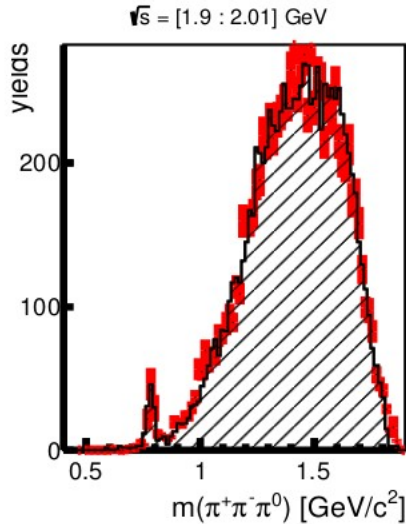
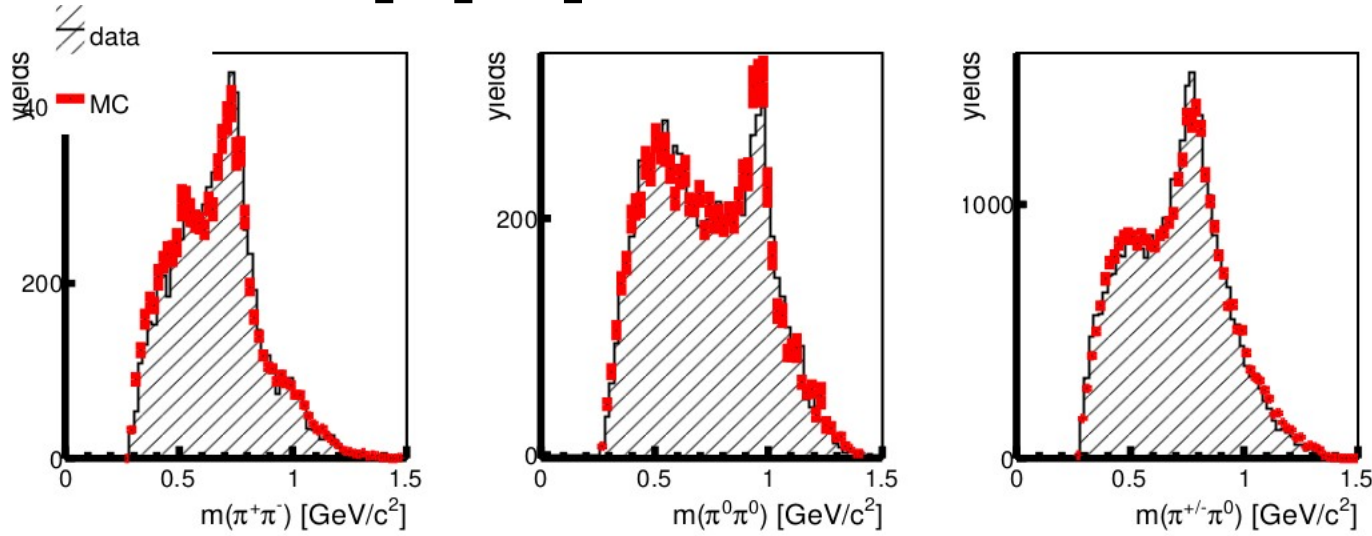
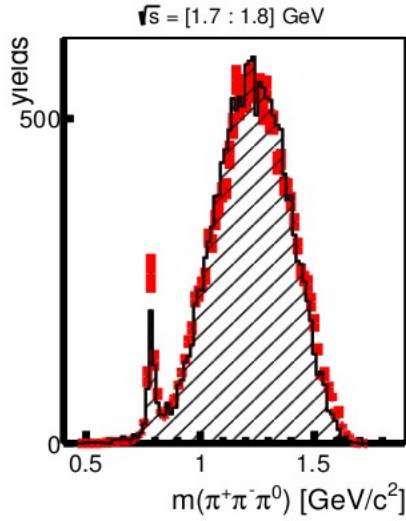
phase



$e^+e^- \rightarrow \pi^+\pi^-\pi^0\pi^0$

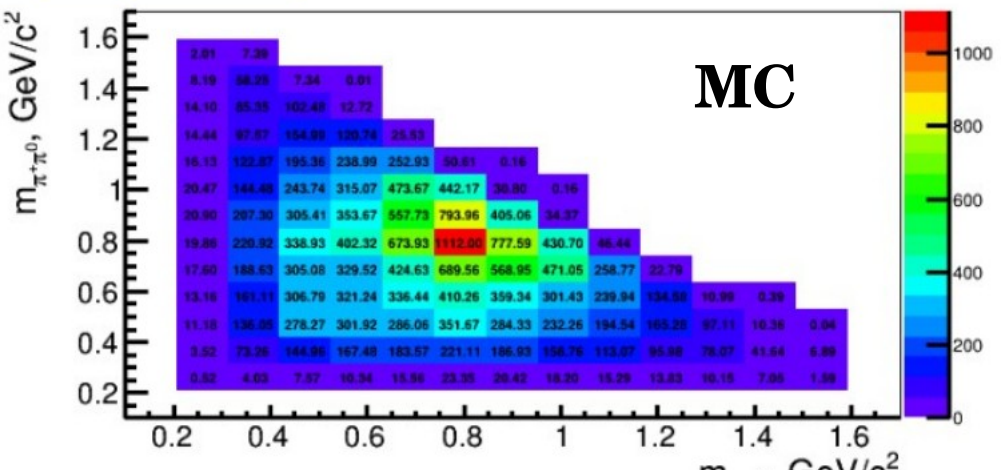
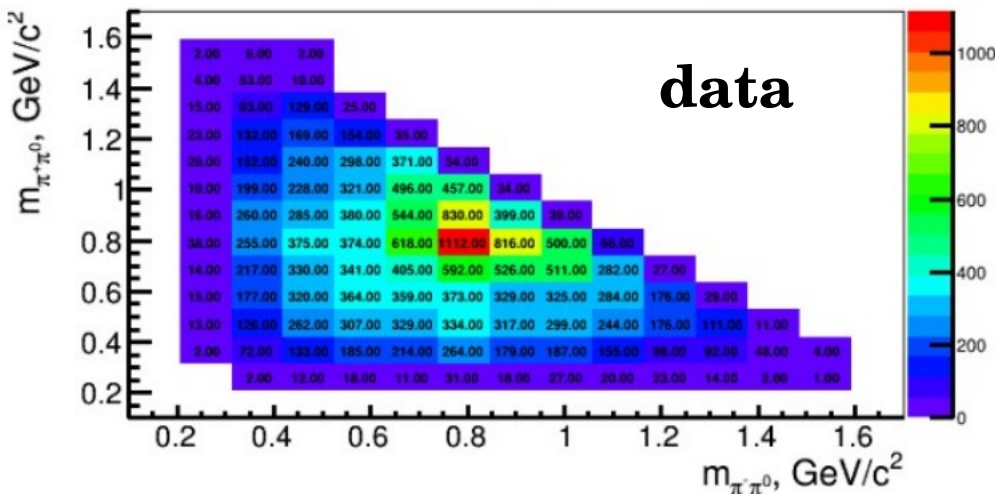


ee \rightarrow pi⁺pi⁻2pi⁰



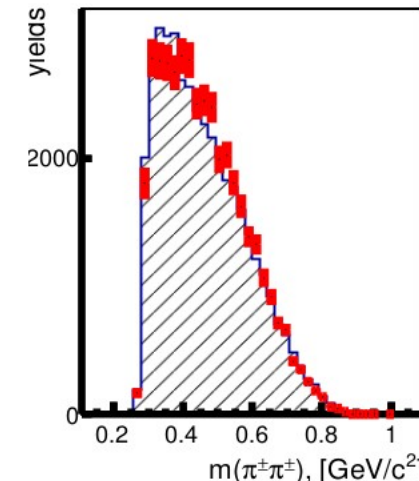
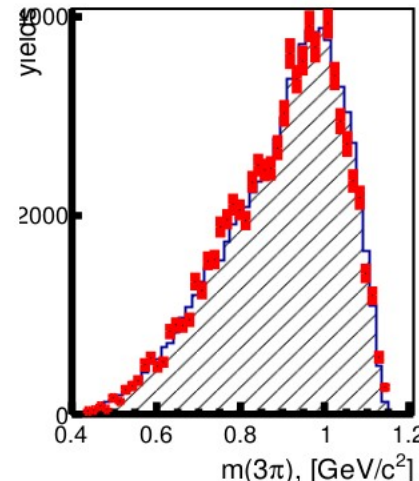
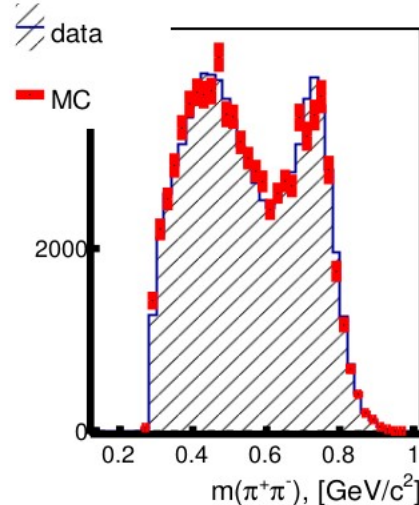
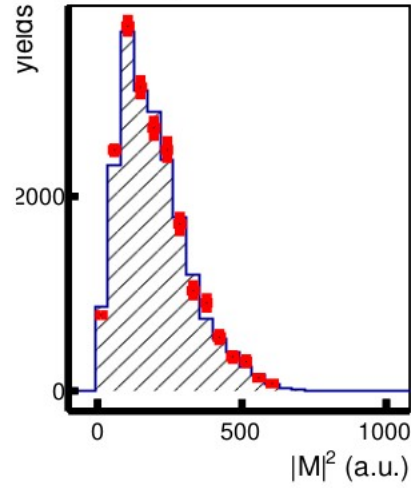
(ee → pi⁺pi⁻2pi⁰)

1.8-1.87654 GeV

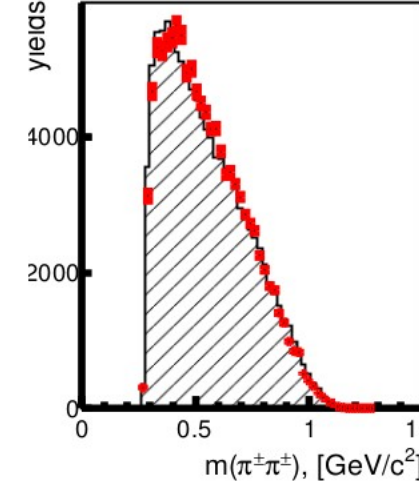
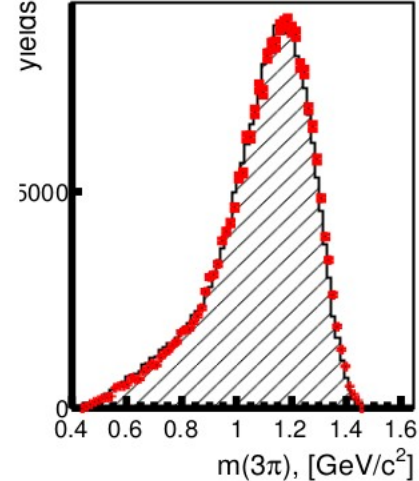
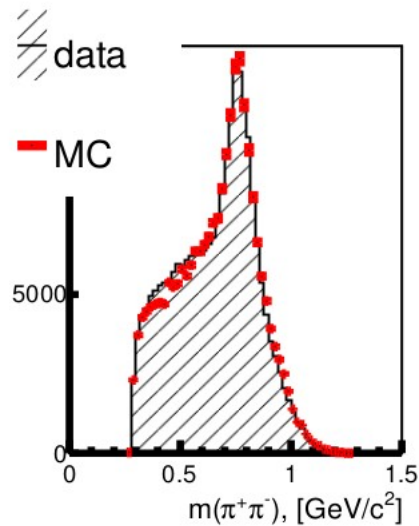
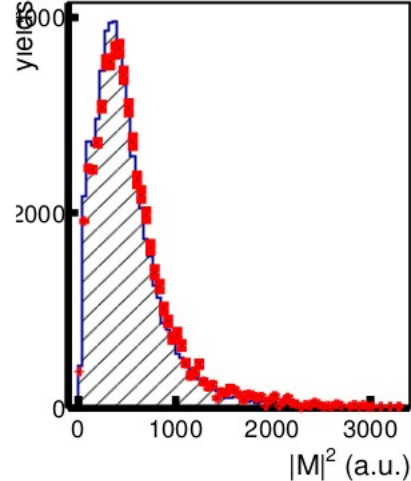


ee \rightarrow 2pi⁺2pi⁻

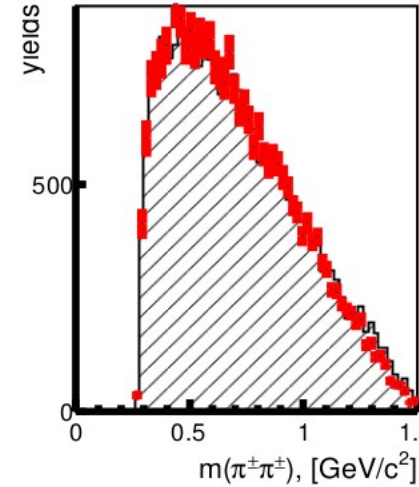
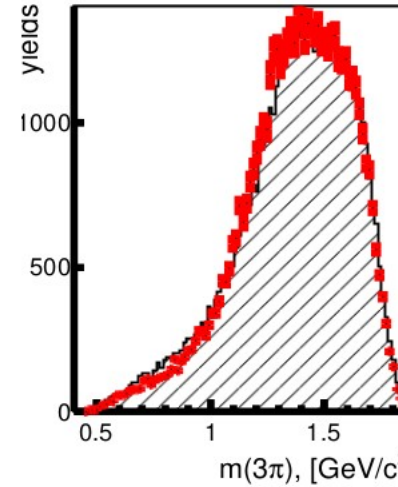
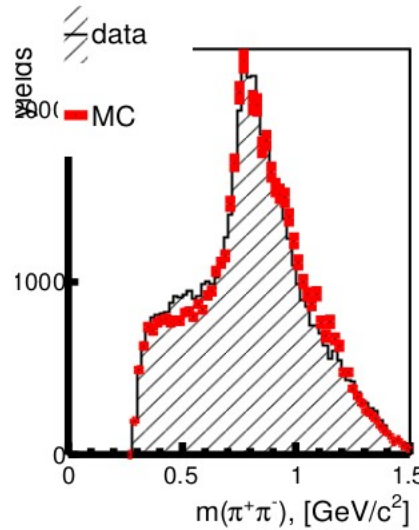
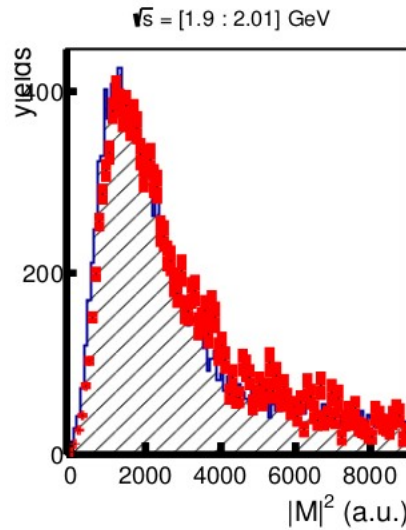
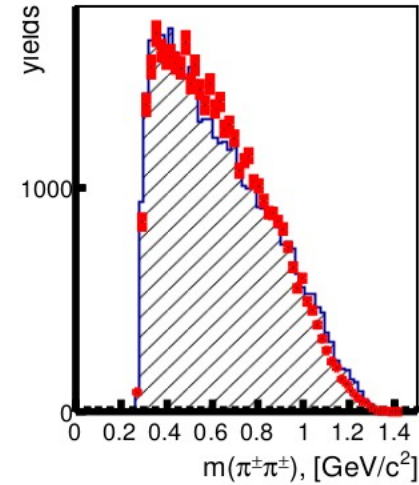
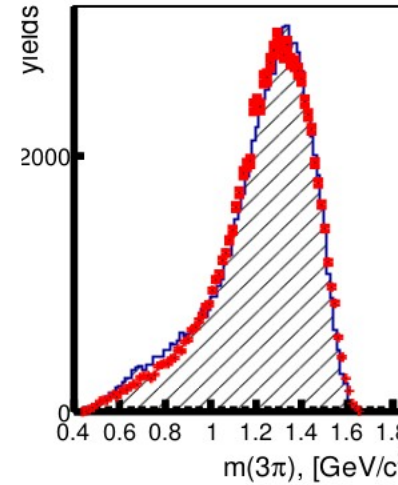
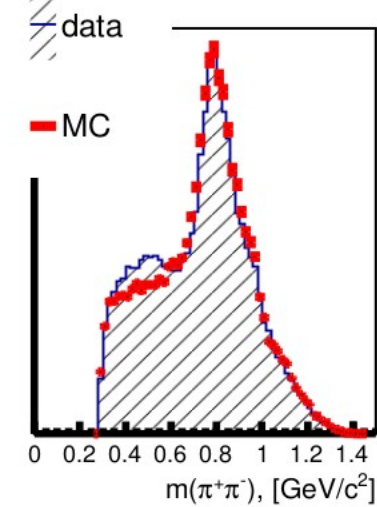
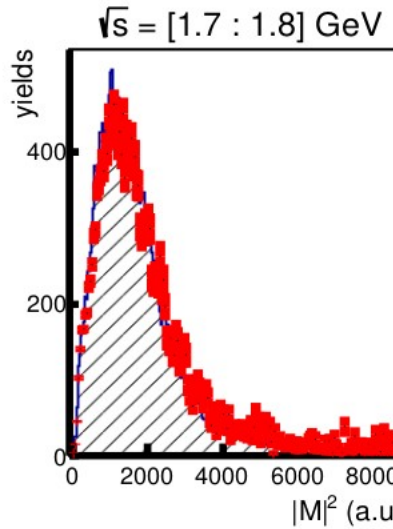
$\sqrt{s} = [1.2 : 1.3] \text{ GeV}$



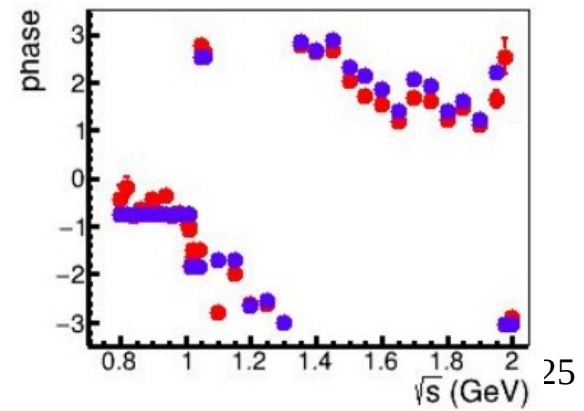
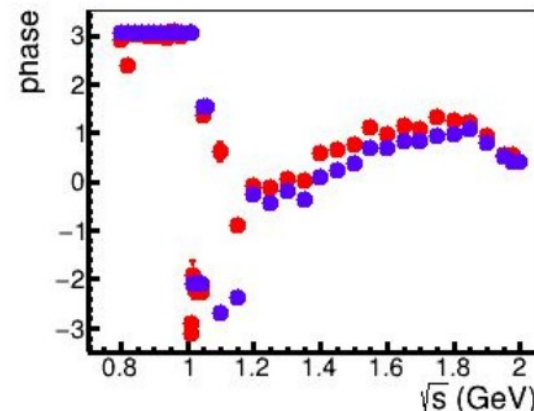
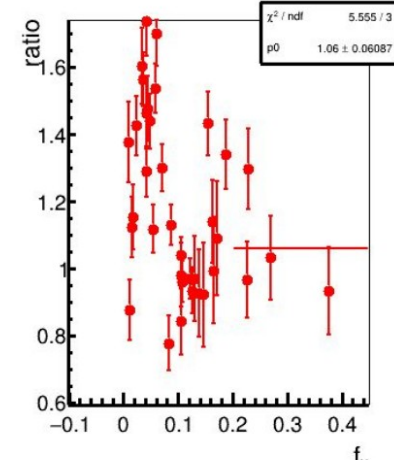
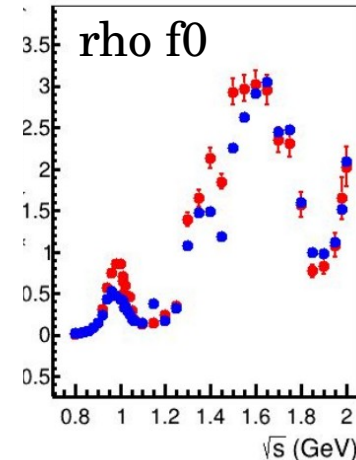
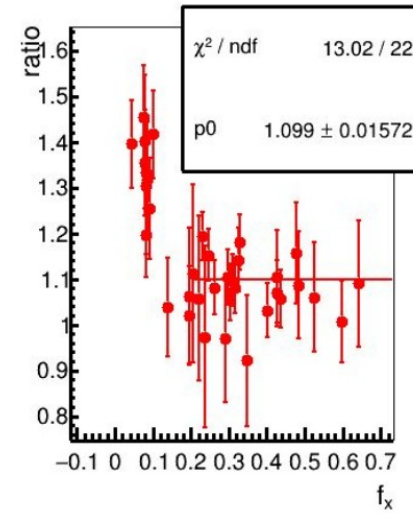
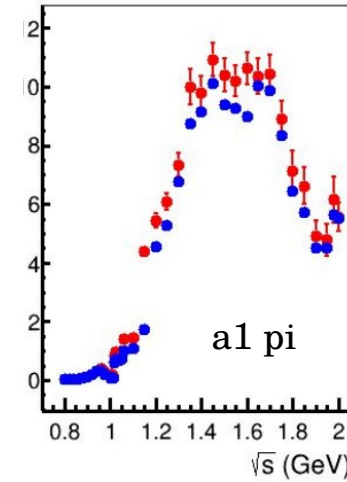
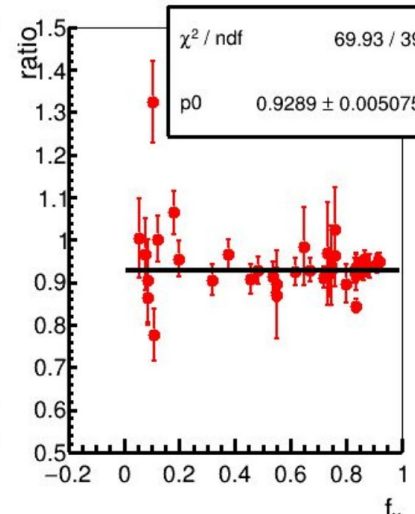
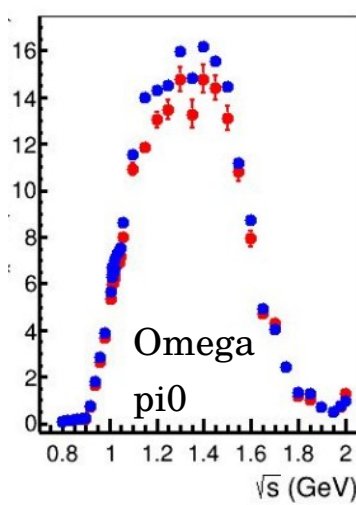
$\sqrt{s} = [1.5 : 1.6] \text{ GeV}$



ee \rightarrow 2pi⁺2pi⁻

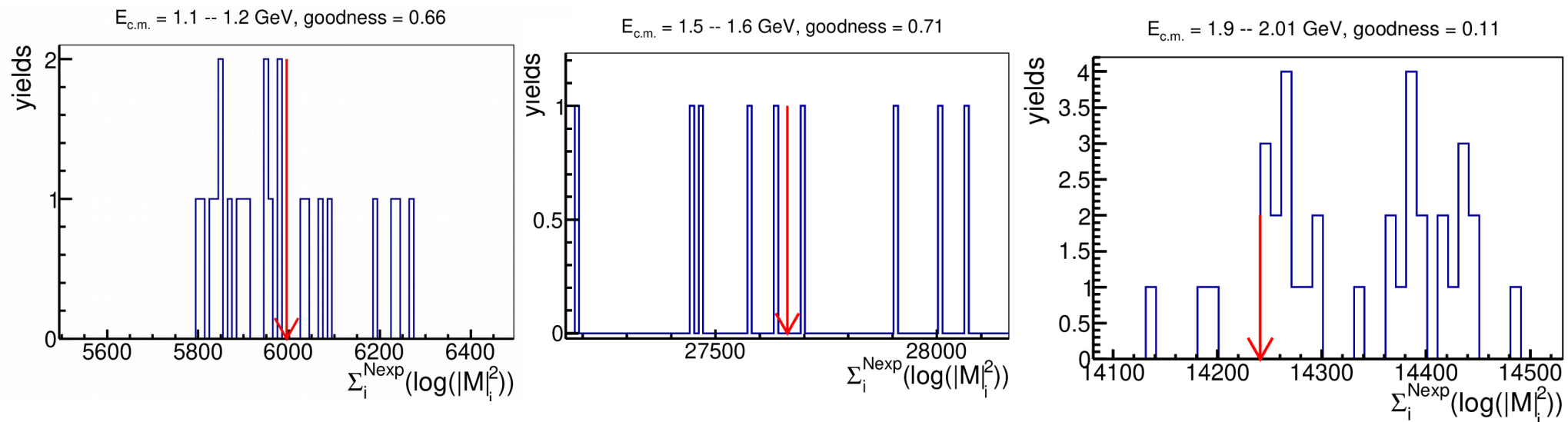


Systematic uncertainty due to detector resolution and ISR is controlled by TOY MC



Goodness-of-fit

We generate 10-30 toy Monte Carlo samples at each energy point. Each sample is generated with parameters obtained in the fit to the data and the number of events in each sample is equal to that observed in the data. The **goodness-of-fit** is estimated as a fraction of samples where $\sum_i^{N_{\text{exp}}} (\log|M_i|^2)$ is less than in the data, where $M = |\sum_\alpha \mathbf{V}_\alpha A_\alpha(\Omega_k)|^2$ - is the total matrix element of the $e^+ e^- \rightarrow 4\pi$.



$$\frac{d\Gamma(J/\psi \rightarrow \pi^0\pi^0\gamma)}{dm} = \omega^3 \frac{1}{8\pi^2} m \rho_{\pi^0\pi^0}(m) \left| \frac{1}{\Delta(m)} \right|^2$$

$$\times \left| g_{gg\sigma} D_{f_0}(m) g_{\sigma\pi^0\pi^0} + g_{gg\sigma} \Pi_{\sigma f_0}(m) g_{f_0\pi^0\pi^0} \right. \\ \left. + g_{ggf_0} \Pi_{f_0\sigma}(m) g_{\sigma\pi^0\pi^0} + g_{ggf_0} D_\sigma(m) g_{f_0\pi^0\pi^0} \right|^2,$$

$$\Delta(m) = D_\sigma(m)D_{f_0}(m) - \Pi_{\sigma f_0}(m)\Pi_{f_0\sigma}(m).$$

$$D_\sigma(m) = m_\sigma^2 - m^2 + \text{Re}(\Pi_\sigma(m_\sigma)) - \Pi_\sigma(m) \text{ and}$$

$$D_{f_0}(m) = m_{f_0}^2 - m^2 + \text{Re}(\Pi_{f_0}(m_{f_0})) - \Pi_{f_0}(m)$$

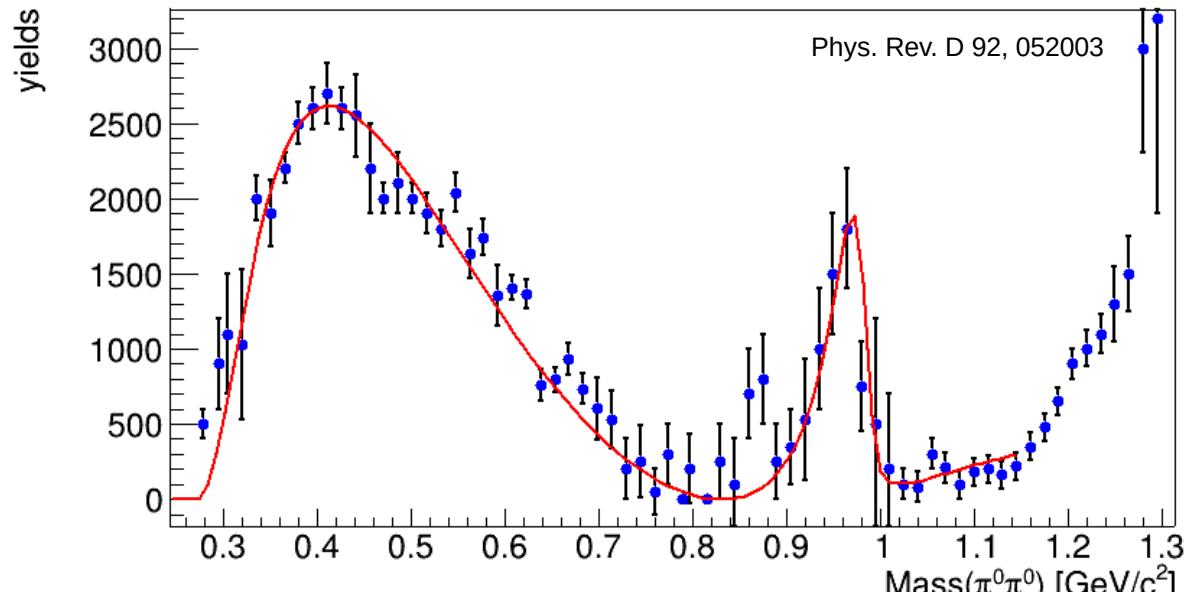
$$\Pi_S(m) = \Pi_S^{\pi\pi}(m) + \Pi_S^{K\bar{K}}(m) + \Pi_S^{\eta\eta}(m)$$

For $m \geq 2m_\pi$

$$\Pi_S^{\pi\pi}(m) = \frac{3}{2} \frac{g_{S\pi\pi}^2}{16\pi} \rho_{\pi\pi}(m) \left(i + \frac{1}{\pi} \ln \frac{1 - \sqrt{1 - 4m_\pi^2/m^2}}{1 + \sqrt{1 + 4m_\pi^2/m^2}} \right),$$

For $m < 2m_\pi$

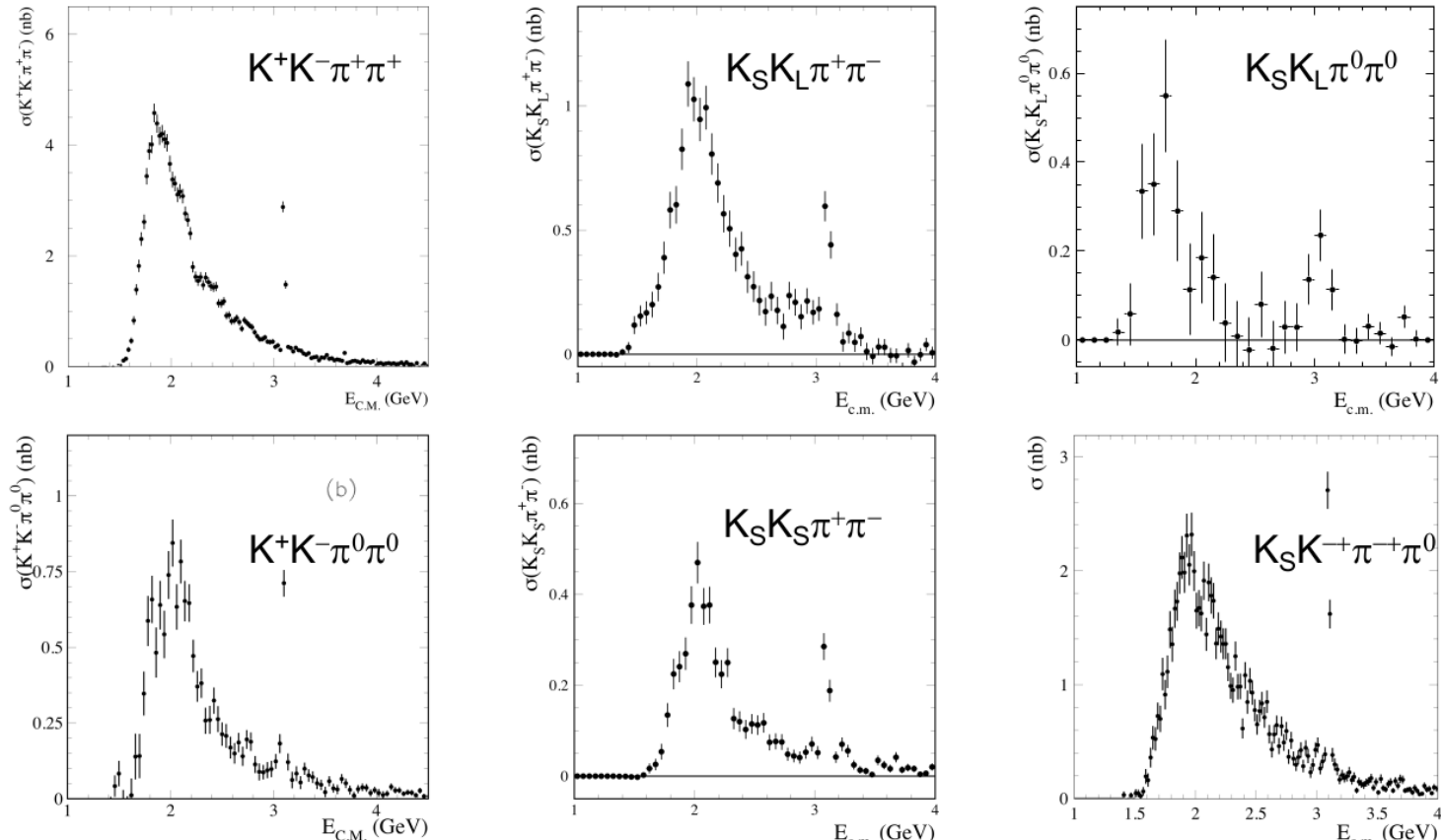
$$\Pi_S^{\pi\pi}(m) = -\frac{3}{2} \frac{g_{S\pi\pi}^2}{16\pi} \sqrt{4m_\pi^2/m^2 - 1} \left(1 - \frac{2}{\pi} \arctan \sqrt{4m_\pi^2/m^2 - 1} \right)$$



$$\Pi_{\sigma f_0}(m) = \Pi_{f_0\sigma}(m) = \Pi_\sigma^{\pi\pi}(m) \frac{g_{f_0\pi\pi}}{g_{\sigma\pi\pi}} + \Pi_{f_0}^{K\bar{K}}(m) \frac{g_{\sigma K\bar{K}}}{g_{f_0 K\bar{K}}}$$

$$+ \Pi_\sigma^{\eta\eta}(m) \frac{g_{f_0\eta\eta}}{g_{\sigma\eta\eta}} + C_{\sigma f_0}$$

All possible $KK\pi\pi$ combinations are measured – BaBar data

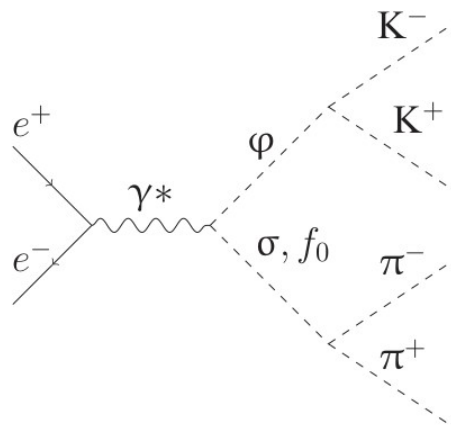
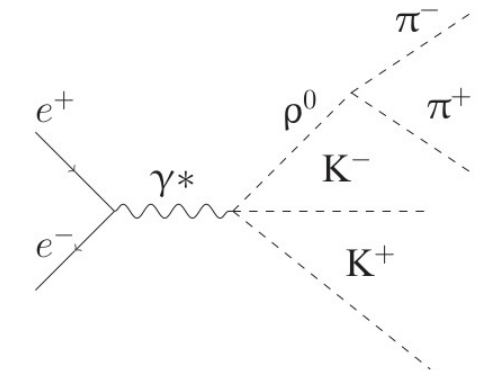
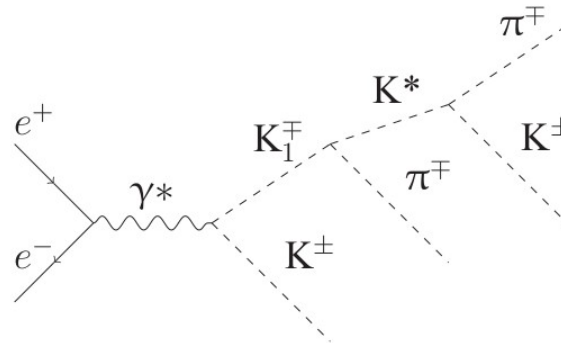
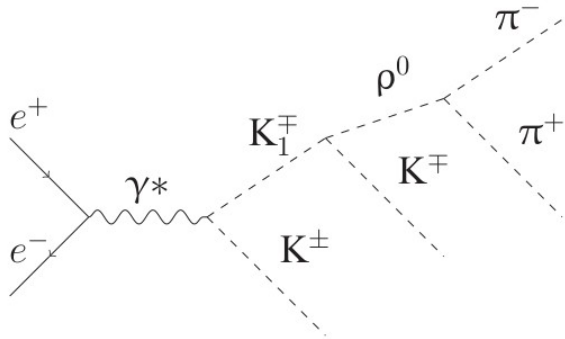


Contribution to $(g-2)_\mu$: (10^{-10} units)

using iso-spin $1.35 \pm 0.09 \pm 0.38 \pm 0.03$ direct 2.41 ± 0.11 $\sqrt{s} < 2.0 \text{ GeV}$

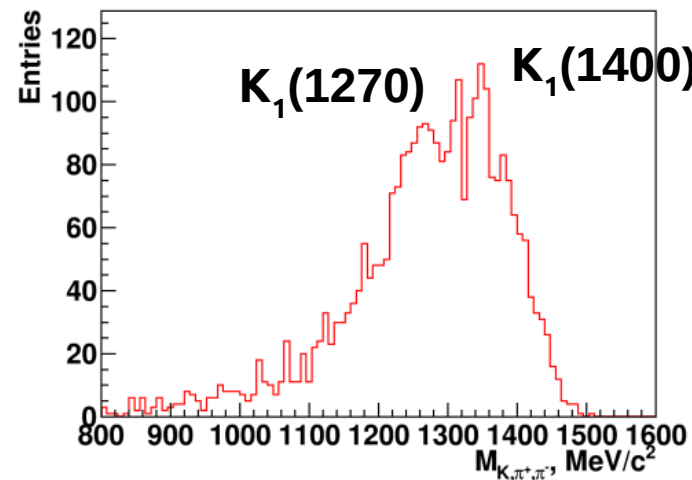
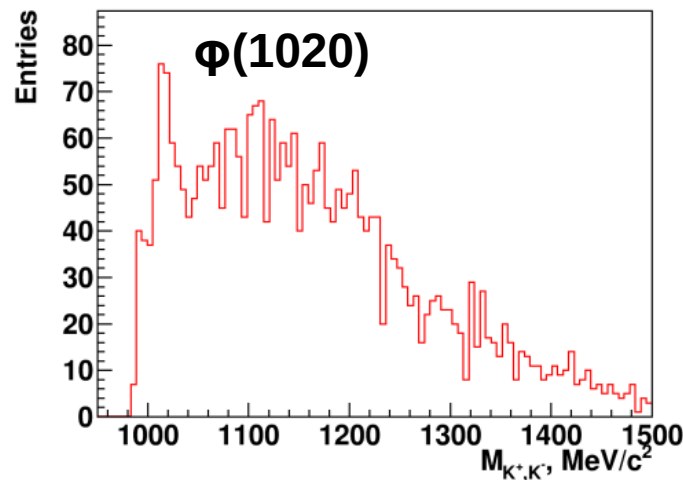
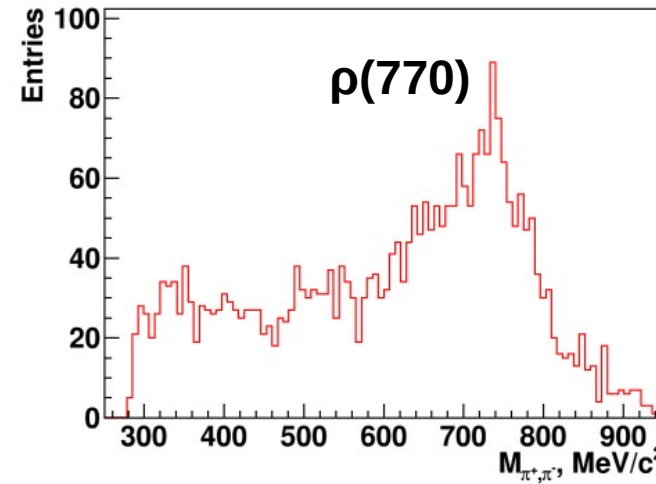
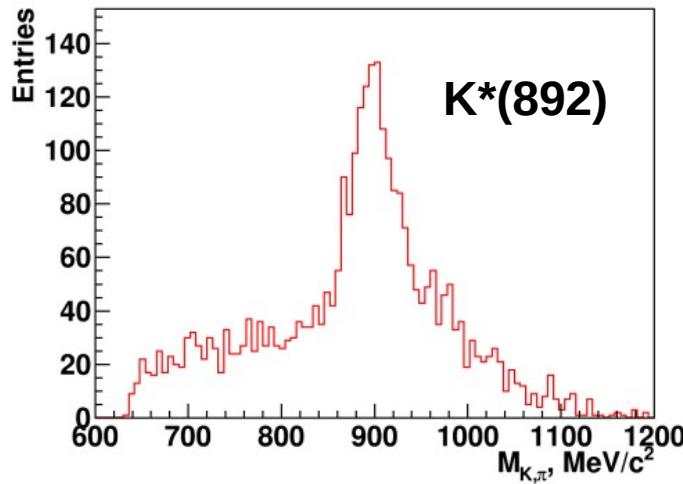
$$\sigma(K\bar{K}\pi\pi) = 9[\sigma(K^+K^-2\pi^0) - \sigma(\phi 2\pi^0)] + \frac{9}{4}\sigma(K^{*0}K^\pm\pi^\mp) + \frac{3}{2}\sigma(\phi\pi^+\pi^-) + 4\sigma(K^+K^-\rho^0).$$

The most important diagrams for the analysis of $e^+e^- \rightarrow K^+K^-\pi^+\pi^-$

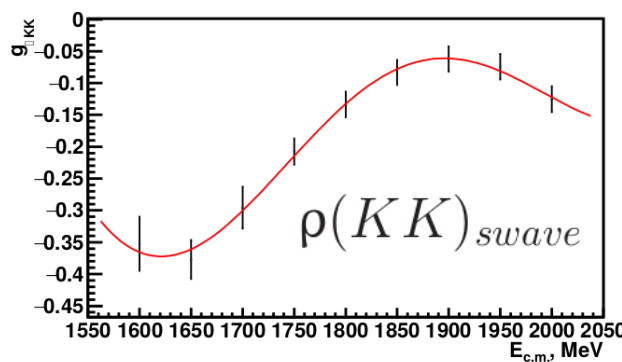
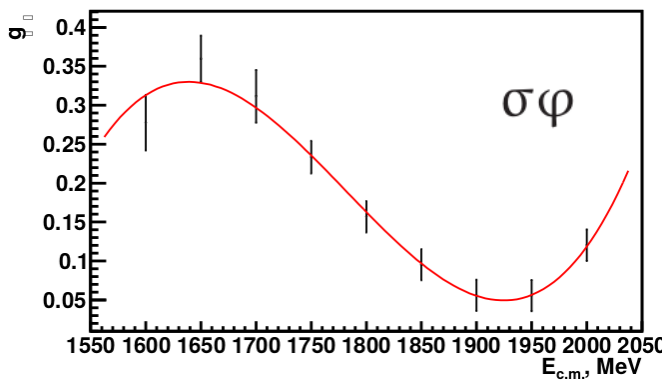
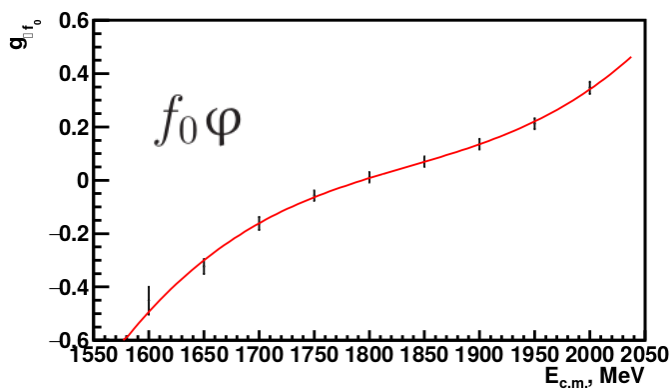
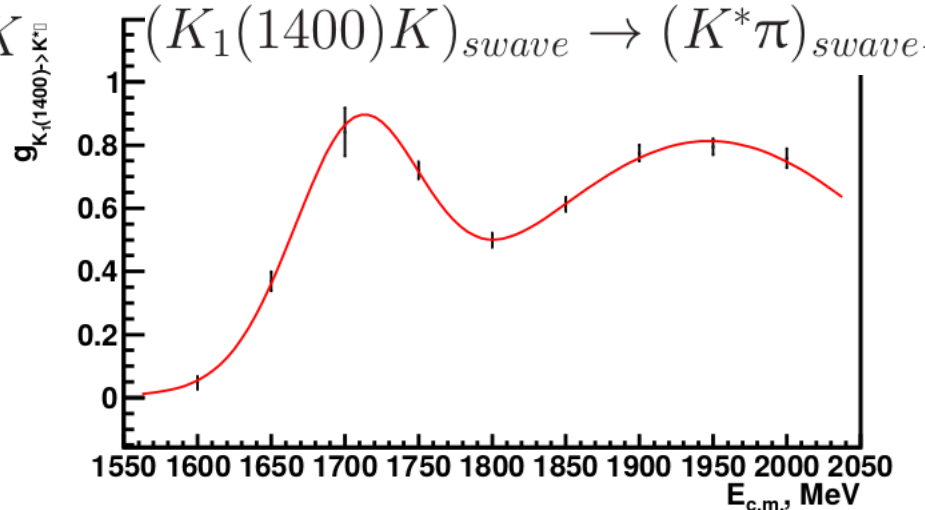
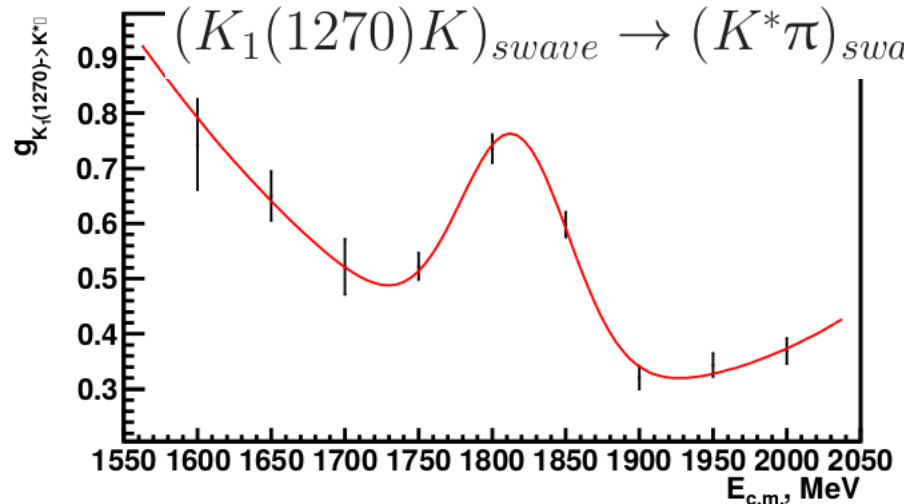


- $e^+e^- \rightarrow (K_1(1270)K)_{swave} \rightarrow (K^*\pi)_{swave}K \rightarrow K\pi\pi K$
- $e^+e^- \rightarrow (K_1(1400)K)_{swave} \rightarrow (K^*\pi)_{swave}K \rightarrow K\pi\pi K$
- $e^+e^- \rightarrow (K_1(1270)K)_{swave} \rightarrow (\rho K)_{swave}K \rightarrow \pi\pi K K$
- $e^+e^- \rightarrow f_0\varphi \rightarrow \pi\pi K K$
- $e^+e^- \rightarrow \sigma\varphi \rightarrow \pi\pi K K$
- $e^+e^- \rightarrow \rho(KK)_{swave}$

Invariant mass spectra for $e^+e^- \rightarrow K^+K^-\pi^+\pi^-$ (10 kevents)

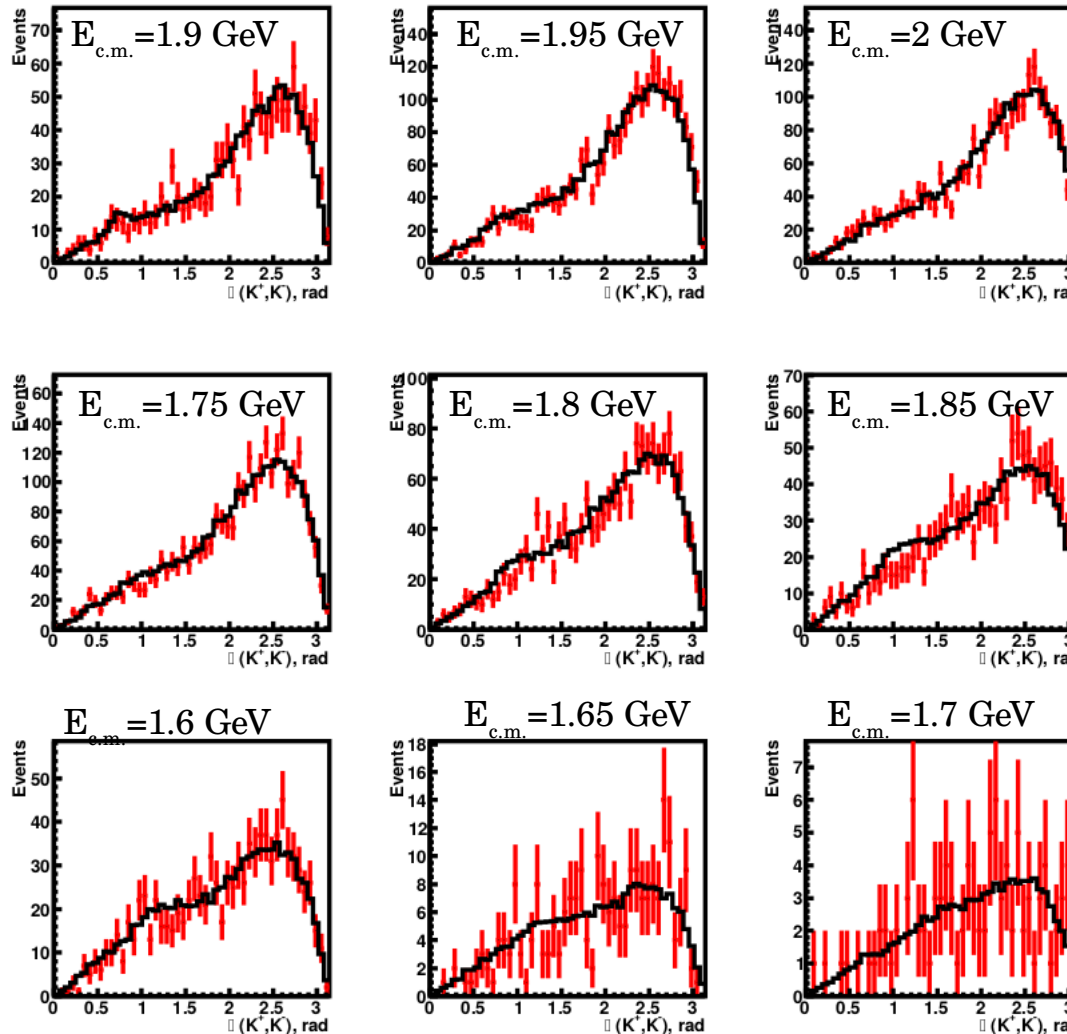


The constant of the amplitudes relatively to $e^+e^- \rightarrow (K_1(1270)K)_{\text{swave}} \rightarrow (\rho K)_{\text{swave}} K \rightarrow KK\pi\pi$



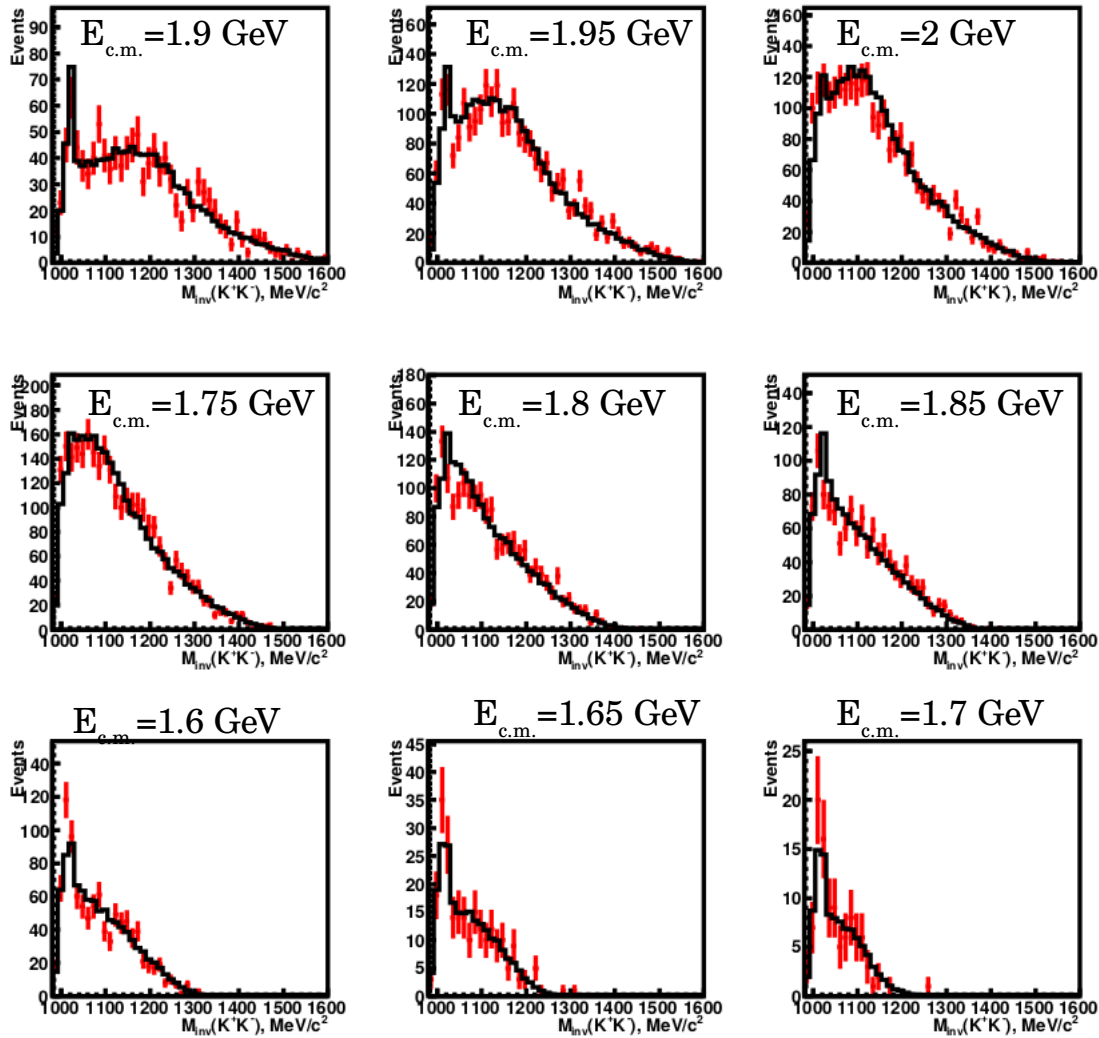
The angle between kaons

EXP
MC



Invariant mass of K+K-

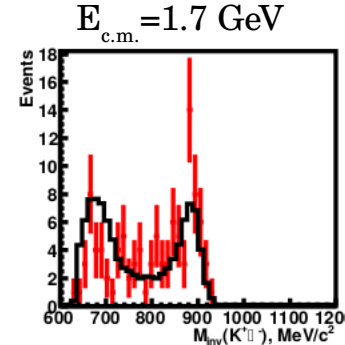
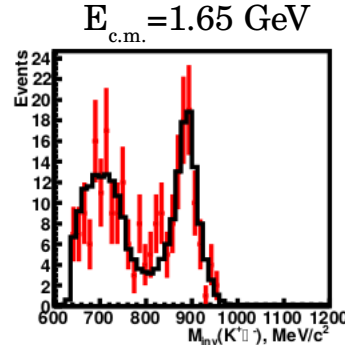
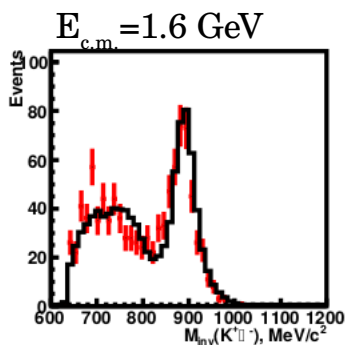
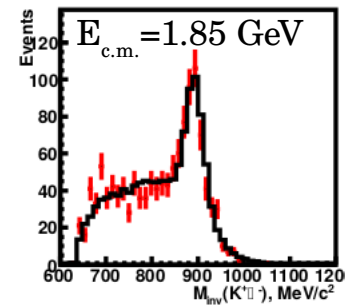
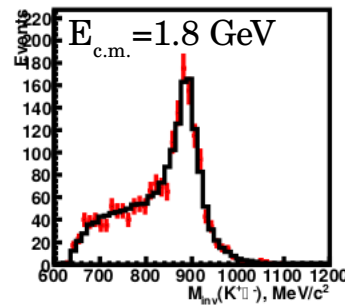
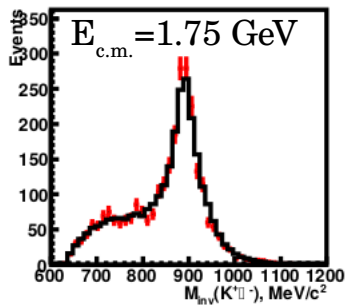
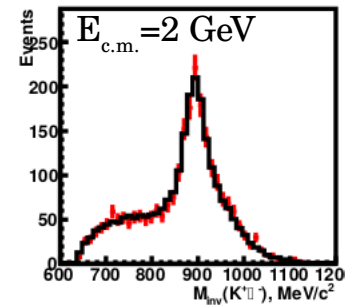
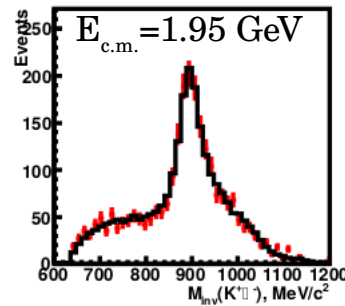
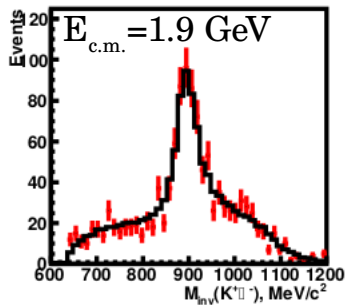
EXP
MC



Invariant mass of πK

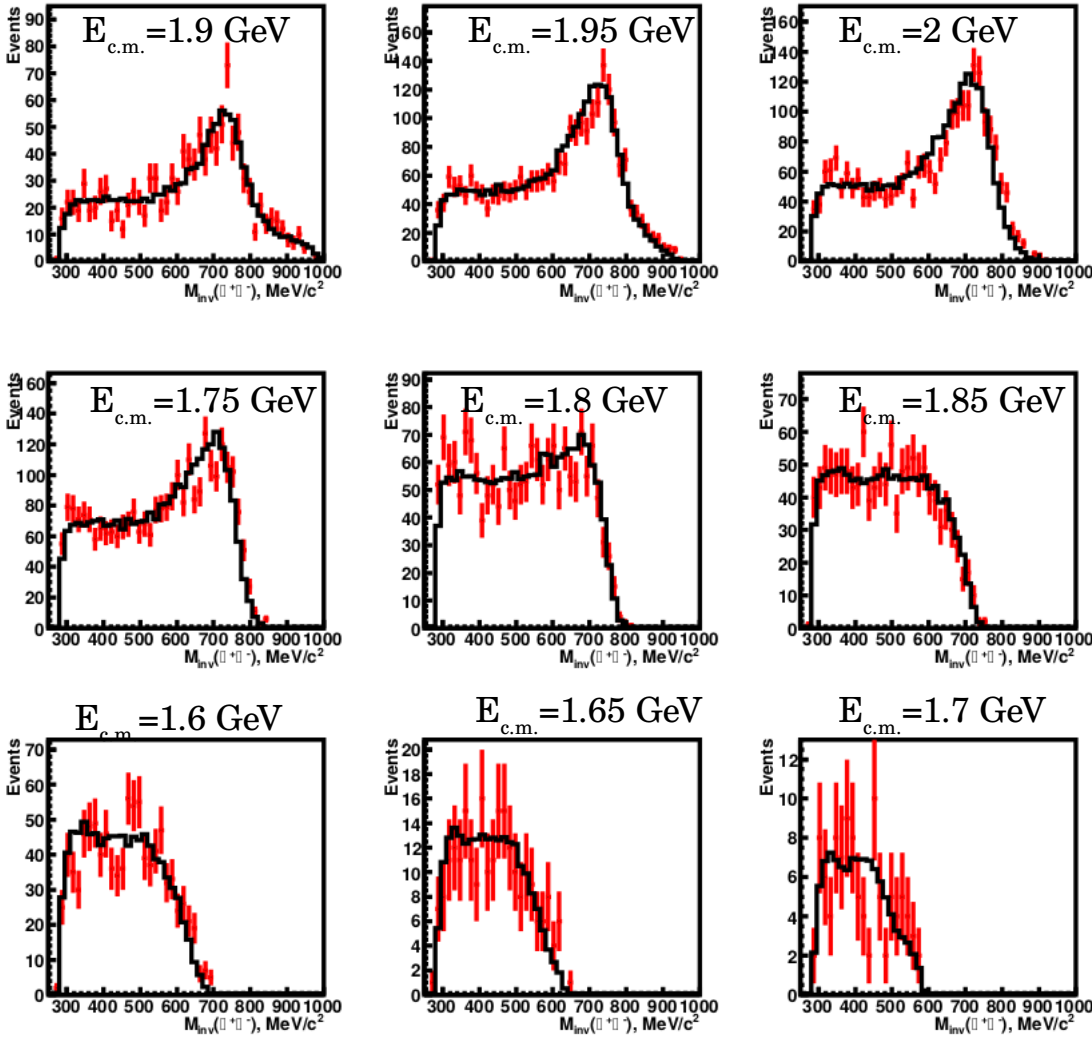
EXP

MC

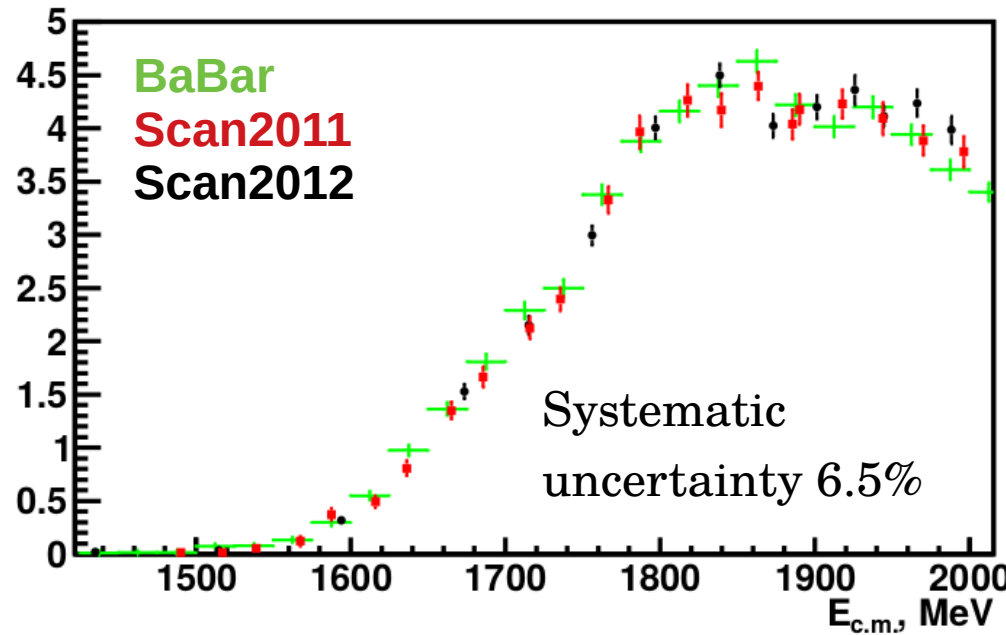


Invariant mass of 2π

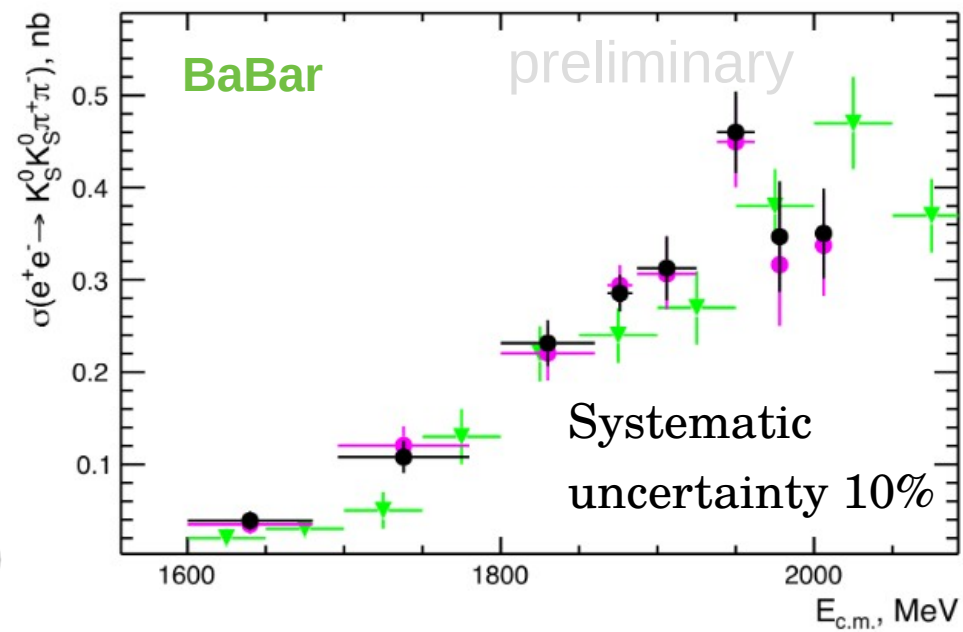
EXP
MC



Cross section of $e^+e^- \rightarrow K^+K^-\pi^+\pi^-$



Cross section of $e^+e^- \rightarrow K_S K_S \pi^+\pi^-$



This reaction is dominated by $K^{*+}(892)K^{*-}(892)$ production

- Simultaneous analysis of all $e^+e^- \rightarrow KK\pi\pi$ channels is required for comprehensive meson spectroscopy and the test of isospin relations

Summary

- The dominance of the channels $\omega\pi$ and $a_1\pi$ below 2 GeV is confirmed in the $e^+e^- \rightarrow 4\pi$. The $\omega\pi$ channel is dominated in the process $e^+e^- \rightarrow \pi^+\pi^-2\pi^0$ up to $\sqrt{s} \sim 1.5$ GeV
- The estimation of the contributions of $\rho\sigma$, ρf_0 , $\rho^-\rho^+$, ρf_2 , $h_1\pi$ is presented
- The perspectives of the analysis of $e^+e^- \rightarrow KK\pi\pi$ is shown
- It looks that the production of two ground-state vectors ($\rho^-\rho^+$, $K^*(890)\bar{K}^*(890)$) is suppressed relatively to the emission of pseudoscalar ($\omega\pi$, $a_1\pi$, K_1K).
- **If you are interesting in the analysing of the CMD-3 data you are more than welcome**